# EXO70A2 Is Critical for Exocyst Complex Function in Pollen Development[1][OPEN]

**Vedrana Marković,[a,b] Fatima Cvrčková,[a] Martin Potocký,[a,b] Ivan Kulich,[a,2] Přemysl Pejchar,[b] Eva Kollárová,[a] Lukáš Synek,[b,3] and Viktor Žárský[a,b,3,4]**

[a]Department of Experimental Plant Biology, Faculty of Science, Charles University, 12844 Prague 2, Czech Republic

[b]Institute of Experimental Botany, Czech Academy of Sciences, 16502 Prague 6, Czech Republic

**ORCID IDs: 0000-0002-0310-5102 (V.M.); 0000-0002-5560-8473 (F.C.); 0000-0002-3699-7549 (M.P.); 0000-0002-0458-6470 (I.K.); 0000-0003-0488-7465 (P.P.); 0000-0003-2709-9461 (E.K.); 0000-0003-2111-2450 (L.S.); 0000-0002-5301-0339 (V.Ž.).**

Pollen development, pollen grain germination, and pollen tube elongation are crucial biological processes in angiosperm plants that need precise regulation to deliver sperm cells to ovules for fertilization. Highly polarized secretion at a growing pollen tube tip requires the exocyst tethering complex responsible for specific targeting of secretory vesicles to the plasma membrane. Here, we demonstrate that Arabidopsis (*Arabidopsis thaliana*) EXO70A2 (At5g52340) is the main exocyst EXO70 isoform in the male gametophyte, governing the conventional secretory function of the exocyst, analogous to EXO70A1 (At5g03540) in the sporophyte. Our analysis of a CRISPR-generated *exo70a2* mutant revealed that EXO70A2 is essential for efficient pollen maturation, pollen grain germination, and pollen tube growth. GFP:EXO70A2 was localized to the nucleus and cytoplasm in developing pollen grains and later to the apical domain in growing pollen tube tips characterized by intensive exocytosis. Moreover, EXO70A2 could substitute for EXO70A1 function in the sporophyte, but not vice versa, indicating partial functional redundancy of these two closely related isoforms and higher specificity of EXO70A2 for pollen development-related processes. Phylogenetic analysis revealed that the ancient duplication of EXO70A, one of which is always highly expressed in pollen, occurred independently in monocots and dicots. In summary, EXO70A2 is a crucial component of the exocyst complex in Arabidopsis pollen that is required for efficient plant sexual reproduction.

The pollen tube in angiosperms represents an extremely elongated cellular structure that emerges from a rehydrated pollen grain when it lands on a stigma and delivers two sperm cells to fertilize an ovule. To reach the ovule, the pollen tube navigates through pistil tissues by highly polarized tip growth, restricted to the pollen tube apex. In this tightly regulated process, cell polarity maintenance mechanisms, addition of new membrane material, and secretion of cell wall components are essential. Intensive exocytosis is localized to the very tip, followed by a subapical domain where endocytosis takes place to recycle the excess of membranes delivered in secretory vesicles (for review, see Hepler and Winship, 2015). Other key factors essential for the pollen tube tip growth include small GTPases and a $Ca^{2+}$-signaling network that regulates actin cytoskeleton dynamics (for review, see Cai et al., 2015). The cell wall of pollen tubes has a unique structure consisting of two layers: a pectinaceous and cellulose layer secreted at the apex, and an additional callose layer deposited in regions more distant from the tip. The spatial distribution of the cell wall components plays a critical role in pollen tube morphogenesis (Chebli et al., 2012). Because pollen tubes are a simplified cell-autonomous system and exhibit highly polarized growth, they provide an excellent model in cell biology for studies of cell polarity and regulation of secretion (e.g. Chebli et al., 2013; Qin and Dong, 2015). Precisely regulated membrane trafficking is crucial not only for pollen tube growth, but also for previous stages of pollen development, namely pollen grain maturation

[1]This work was supported by the Czech Science Foundation (project no. 18–18290J) and the Ministry of Education, Youth and Sports of the Czech Republic, supported by the European Regional Development Fund project "Centre for Experimental Plant Biology" (grant no. CZ.02.1.01/0.0/0.0/16_019/0000738 to V.M. and V.Z.), the state budget of the Czech Republic (grant nos. CZ.1.05/4.1.00/16.0347 and CZ.2.16/3.1.00/21515), the Operational Programme Prague – Competitiveness (grant no. OPPK CZ.2.16/3.1.00/21519), and a large-RI project (grant no. LM2015062 Czech-BioImaging).

[2]Present address: Cell Biology and Plant Biochemistry, University of Regensburg, Universitätsstraße 31, 93053 Regensburg, Germany.

[3]Senior authors.

[4]Author for contact: viktor.zarsky@natur.cuni.cz.

The author responsible for distribution of materials integral to the findings presented in this article in accordance with the policy described in the Instructions for Authors (www.plantphysiol.org) is: Viktor Žárský (viktor.zarsky@natur.cuni.cz).

V.M., L.S., I.K., and V.Z. planned and designed the research; V.M., L.S., P.P., and E.K. performed biological experiments; F.C. and M.P. conducted the phylogenetic analysis; and V.M., L.S., F.C., and V.Z. wrote the manuscript.

[OPEN]Articles can be viewed without a subscription.

www.plantphysiol.org/cgi/doi/10.1104/pp.19.01340

  

and germination (Kang et al., 2003; Peng et al., 2011; Paul et al., 2016).

One of the fundamental regulators of polarized secretion is the exocyst—an evolutionarily conserved protein complex discovered due to its role in docking and tethering of secretory vesicles to specific sites at the plasma membrane (PM), facilitating subsequent fusion of secretory vesicles with the target membrane mediated by SNARE proteins. The exocyst, first described in yeasts and mammals, consists of eight subunits, Sec3, Sec5, Sec6, Sec8, Sec10, Sec15, Exo70, and Exo84 (TerBush et al., 1996; Guo et al., 1999), with Sec3 and Exo70 generally believed to be responsible for targeting the complex to the PM, while the other subunits form the core of the complex (Boyd et al., 2004; He et al., 2007; Pleskot et al., 2015). Plant genomes encode all exocyst subunits (Cvrčková et al., 2001; Elias et al., 2003) that form a functional complex (Hála et al., 2008; Fendrych et al., 2010) and engage in cellular processes requiring polarized secretion, including root hair and pollen tube elongation (Cole et al., 2005; Synek et al., 2006; Hála et al., 2008; Synek et al., 2017), cytokinesis (Fendrych et al., 2010; Rybak et al., 2014), secondary cell wall deposition in trichomes and during xylem development (Kulich et al., 2015; Kubátová et al., 2019; Vukašinović et al., 2017), localized deposition of seed coat pectins (Kulich et al., 2010), transport of PIN auxin carriers to the PM (Drdová et al., 2013), and response to pathogens (Pečenková et al., 2011; Sabol et al., 2017). Viable Arabidopsis (*Arabidopsis thaliana*) mutants defective in exocyst subunits (*sec8-4*, *sec15b*, *exo70a1*, and *exo84b*) exhibit dwarfish growth with pleiotropic developmental defects (Cole et al., 2005; Synek et al., 2006; Hála et al., 2008; Fendrych et al., 2010; Janková Drdová et al., 2019; K. Batystová, M. Klejchová, E. Janková Drdová, L. Synek, P. Sabol, M. Potocký, V. Žárský, and M. Hála, unpublished data).

While in yeast and animals the exocyst subunits are typically encoded by a single gene, in land plants they are usually duplicated or even multiplied (Elias et al., 2003; Cvrčková et al., 2012), with extreme gene proliferation in the case of the EXO70 subunit. For example, the genome of *Physcomitrella patens* encodes 13 *EXO70* paralogs, that of *Oryza sativa* 47 paralogs, and that of Arabidopsis 23 paralogs, which can be divided into three clades of ancestral land plant origin, termed EXO70.1, EXO70.2, and EXO70.3 (Cvrčková et al., 2012; Rawat et al., 2017; Žárský et al., 2020). This plant-specific multiplicity of EXO70 suggests not only functional specialization in different plant tissues or cell types, but also a presence of several variants of the exocyst complex in the same cell (Žárský et al., 2013). Indeed, some EXO70.2 and EXO70.3 clade members contribute to conventional secretion in specific cell types, whereas several other isoforms acquire functions outside the conventional exocytosis pathway, acting in exocyst subcomplexes or even independently of the exocyst complex in some cases (Kulich et al., 2013, 2015; Zhang et al., 2015; Hong et al., 2016; Pečenková et al., 2017; Synek et al., 2017). In contrast, the Arabidopsis EXO70.1 isoform EXO70A1, highly expressed in most sporophytic tissues, is the main housekeeping EXO70 subunit participating in exocytosis (Synek et al., 2006; Fendrych et al., 2010; Drdová et al., 2013). However, since EXO70A1 is not expressed in pollen, the main EXO70.1 paralog functioning in pollen has remained experimentally uncharacterized until now.

The importance of the exocyst for pollen grain germination and pollen tube growth is well documented. Homozygous Arabidopsis mutants in *SEC5a/b*, *SEC6*, *SEC8*, and *SEC15a* typically produce short and wide pollen tubes with compromised polarity, resulting in a male-specific transmission defect (Cole et al., 2005; Hála et al., 2008), and *sec3a* mutants cannot produce pollen tubes at all (Bloch et al., 2016). Transcriptomic and proteomic analyses documented high transcription of the *EXO70A2*, *EXO70C1*, *EXO70C2*, *EXO70F1*, *EXO70H3*, *EXO70H5*, and *EXO70H6* paralogs in Arabidopsis pollen, whereby EXO70C2, EXO70C1, and EXO70A2 were the most abundant in the Arabidopsis pollen proteome (Grobei et al., 2009, Synek et al., 2017). The two closely related EXO70C1 and EXO70C2 paralogs from the EXO70.2 clade participate in the control of optimal pollen tube tip growth (Synek et al., 2017). Pollen tubes lacking EXO70C2 exhibited aberrant morphology, frequently bursting and displaying a distinct stop-and-go mode of elongation, resulting in a seriously reduced fertilization capacity. These facts point to a divergent function of EXO70C2 (and its close paralog EXO70C1) independent of the conventional exocyst function (Synek et al., 2017). On the other hand, the clade EXO70.1 member EXO70A2 is the evolutionarily closest paralog to EXO70A1, the main sporophytic housekeeping isoform (Cvrčková et al., 2012), which represents the best candidate for the main conventional EXO70 isoform in pollen, functioning as a part of the exocyst complex in the regulation of polarized exocytosis.

In this study, we document that disruption of EXO70A2 in Arabidopsis affects pollen maturation, significantly reduces pollen germination efficiency, and causes a severe pollen-specific transmission defect of the mutant allele, which is at least in part due to impaired pollen tube growth. GFP:EXO70A2 localizes to the nucleus and cytoplasm in developing pollen grains and later to the apical PM domain in growing pollen tubes characterized by intensive exocytosis. Interestingly, ectopic expression of EXO70A2 could substitute for the EXO70A1 function in the sporophyte, but not vice versa, indicating partial functional redundancy of these two closely related isoforms. Phylogenetic and expression analysis of EXO70 genes in the EXO70.1 clade revealed independent duplications of EXO70A in monocots and dicots and showed that the dicot EXO70A2 clade contains predominantly pollen-expressed isoforms. We conclude that Arabidopsis EXO70A2 is the main EXO70 isoform functioning as a subunit of the exocyst complex in conventional secretion in Arabidopsis pollen.

## RESULTS

### EXO70A2 Is a Member of a Dicot Pollen-Expressed EXO70.1 Clade

To clarify the evolutionary relationships among EXO70A paralogs, which comprise the sole family of the ancestral EXO70.1 clade (Synek et al., 2006; Cvrčková et al., 2012; Rawat et al., 2017), we performed a detailed phylogenetic analysis of available predicted protein sequences of members of this clade from 19 plant species covering a broad range of land plant diversity including liverworts, mosses, lycophytes, gymnosperms, the basal angiosperm *Amborella trichopoda*, grasses as representatives of monocots, and representatives of both asterid and rosid eudicot lineages (sequences are listed in Supplemental File S1). The sole EXO70 of the charophyte *Klebsormidium flaccidum* was also included as an outgroup. The resulting phylogenetic tree (Fig. 1) clearly indicates that the EXO70A duplication took place independently in basal eudicots and in monocots (or at least in grasses), resulting in both eudicots and grasses possessing representatives of two EXO70A clades that cannot be considered orthologous between the two angiosperm lineages. The Arabidopsis EXO70A1 and EXO70A2 paralogs map into different eudicot EXO70A clades, whereas the third paralog, EXO70A3, is closely related to EXO70A2 and resulted from a recent gene duplication that may have been restricted to Brassicales, or even to some subgroup thereof.

For selected representatives of both monocots and eudicots, transcript level data for the analyzed genes were extracted from public databases and mapped onto the phylogenetic tree (Fig. 1). The results document clade-specific distinct expression patterns in both eudicots and grasses. In eudicots, members of the clade containing Arabidopsis EXO70A1 usually exhibit high expression levels in sporophytic vegetative organs, with low or no expression in pollen, whereas a complementary pattern, i.e. high transcript level in pollen and lower to no expression in the sporophyte, is typical for the clade containing EXO70A2. Also, in the grasses, one of the two clades contains mostly genes with either ubiquitous or predominantly sporophytic expression, whereas most members of the other exhibit enhanced, though usually not exclusive, expression in the male gametophyte.

### Preparation and Characterization of a Loss-of-Function *exo70a2* Allele Using the CRISPR/Cas9 System

To investigate the function of *EXO70A2* in planta, we intended to use Arabidopsis mutants, but at the time of this study, T-DNA insertion null mutants in *EXO70A2* (At5g52340) were not available. The publicly available GABI_824D06 line (*exo70a2-1*) with an insertion located in the 5′ untranslated region exhibited EXO70A2 overexpression (Synek et al., 2017), and the FLAG_264F01 line could not be confirmed in our hands. We thus employed the CRISPR/Cas9 system (Wang et al., 2015) and targeted it specifically to the *EXO70A2* gene to generate a loss-of-function *exo70a2* mutant in the Arabidopsis ecotype Columbia-0 background. We obtained a mutant line (*exo70a2-4*) bearing a 13-bp insertion in the fifth exon (of 11 exons) of the *EXO70A2* gene that caused a frameshift in the coding sequence, resulting in a premature stop codon (Supplemental Fig. S1A). The insertion likely affected the *EXO70A2* mRNA stability or processing, because the *EXO70A2* transcript level was reduced in the *exo70a2-4* mutant to less than half the wild-type level as evaluated by semiquantitative reverse transcription PCR (RT-sqPCR) in flower material (Supplemental Fig. S1B).

Plants homozygous for the CRISPR-generated insertion (hereafter referred to as *exo70a2*) were then subjected to phenotype analysis and compared to their wild-type counterparts. To address whether EXO70A2 might play some role in the sporophyte despite its minimal expression in sporophytic tissues (Synek et al., 2006; Hruz et al., 2008; www.Genevestigator.com), we inspected the morphology of the mutant and wild-type plants and evaluated two basic morphological parameters. Primary root length of 7-d-old seedlings grown on vertical agar plates was comparable between *exo70a2* and the wild type (Supplemental Fig. S1, C and D). Similarly, 5-week-old *exo70a2* and wild-type plants showed no difference in plant height and general plant morphology (Supplemental Fig. S1, E and F). In conclusion, the sporophyte of *exo70a2* homozygotes was not affected by the mutation, consistent with the notion that EXO70A2 is a key EXO70 isoform functioning in pollen.

### The *exo70a2* Mutant Shows a Pollen-Specific Transmission Defect

We next analyzed the transmission of the *exo70a2* mutant allele through pollen. Based on PCR genotyping, the progeny of heterozygous *exo70a2* mutant plants showed a significantly reduced portion of mutant homozygotes in comparison to the normal Mendelian ratio (only 15% of the tested plants were mutant homozygotes), pointing to a severe transmission defect of this mutant allele (Table 1).

To prove that the transmission defect was specific to males we performed reciprocal crossing of *exo70a2* heterozygotes to wild-type plants and inspected the frequency of wild-type and heterozygous progeny (Table 2). When *exo70a2* heterozygous plants were used as pollen donors, only 17% of the progeny were heterozygous for the *exo70a2* allele instead of the expected 50%. However, when they were used as pollen recipients, 54% of the progeny were heterozygous, indicating that the transmission defect was male specific.

### Pollen Maturation and Germination Are Compromised in the *exo70a2* Mutant

To investigate the nature of the pollen-specific transmission defect, we inspected pollen development,

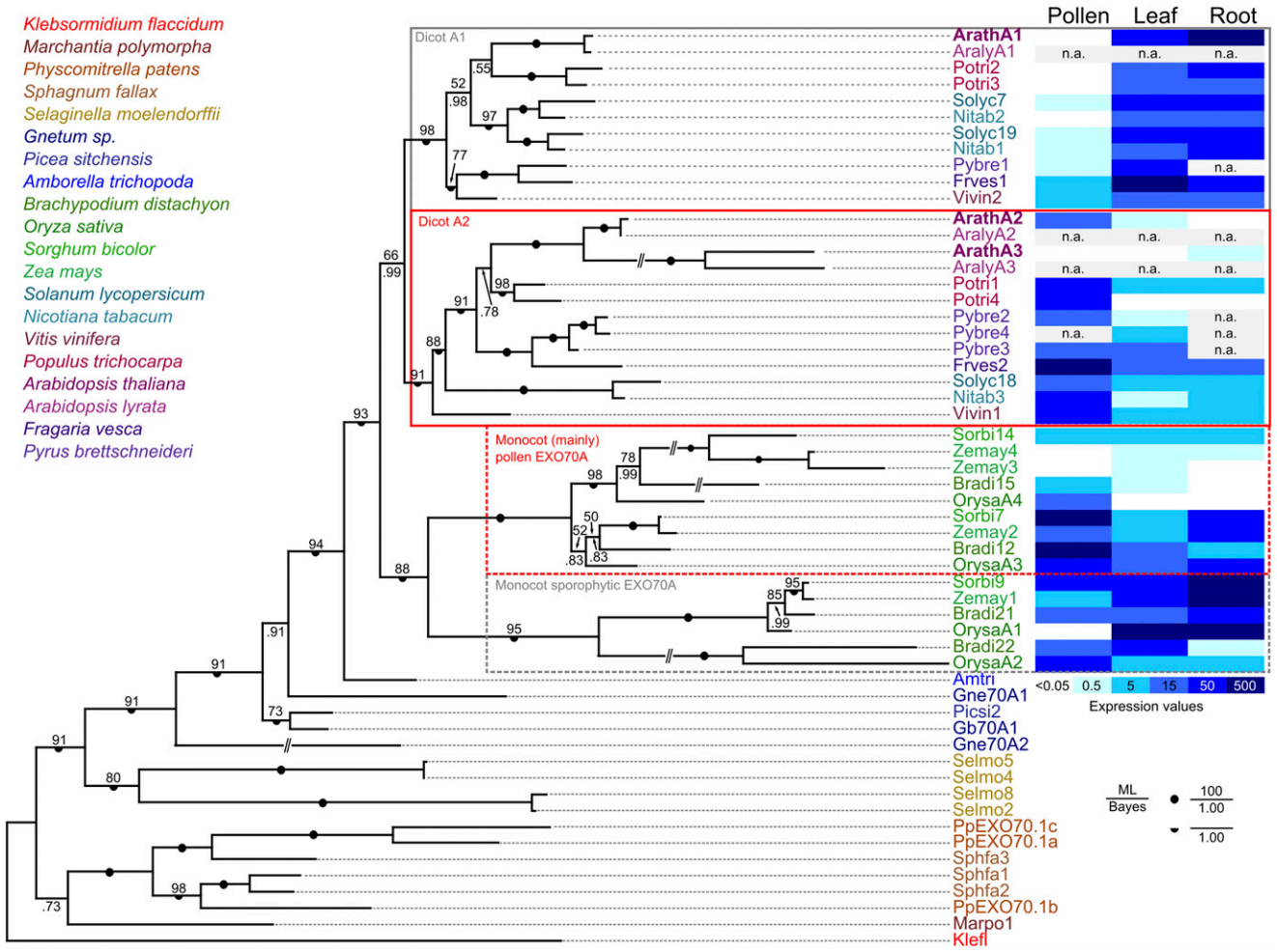


**Figure 1.** Phylogenetic and expression analysis of the EXO70.1 clade in land plants. A Bayesian phylogenetic tree of EXO70.1 protein sequences from representative land plants ranging from liverworts (*Marchantia polymorpha*), mosses (*P. patens* and *Sphagnum fallax*), lycophytes (*Selaginella moelendorffii*), gymnosperms (*Gnetum* sp., *Picea sitchensis*), the basal angiosperm *Amborella trichopoda*, and grasses (*Brachypodium distachyon*, *O. sativa*, *Sorghum bicolor*, and *Zea mays*) as representatives of the monocots, and both asterids (*Solanum lycopersicum* and *Nicotiana tabacum*) and multiple rosids (*Vitis vinifera*, *Populus trichocarpa*, Arabidopsis, *Arabidopsis lyrata*, *Fragaria vesca*, and *Pyrus brettschneideri*) as representatives of the eudicots. The sole EXO70 of the charophyte *Klebsormidium flaccidum* has been included as an outgroup (for a full list of sequences with accessions see Supplemental File S1). A consistent tree was also obtained by the maximum likelihood method (bootstrap values shown); full support for some branches is denoted by symbols. For selected angiosperm species, a heat map of transcript levels in pollen and sporophytic tissues, inferred from publicly available transcriptome data, is shown. ML, Maximum likelihood; n.a., not available.

including pollen germination and pollen tube growth in *exo70a2* and wild-type plants. Initially, we conducted an in vitro pollen germination assay on pollen samples harvested from homozygous *exo70a2* mutants, heterozygous *exo70a2* mutants, and wild-type controls. While the control pollen started to efficiently germinate within 2 h after imbibition, the pollen from *exo70a2* homozygotes germinated no sooner than 8 h after the imbibition (Fig. 2, A and B). Even after 20 h, the *exo70a2* pollen still showed 8-fold lower germination efficiency than wild-type pollen.

In order to resolve the pollen germination defect, we further analyzed pollen grain viability and several aspects of maturation. We observed a four-times-higher percentage of nonviable pollen grains at the mature pollen stage in *exo70a2* compared to the wild type using Alexander staining (wild type, 3.4%, $n$ = 179; *exo70a2*, 11.5%, $n$ = 157; $P$ = 0.004, $\chi^2$ test; Fig. 2C). An analysis of nuclear composition in the pollen using 4′,6-diamino-phenylindole staining demonstrated that *exo70a2* pollen grains could proceed through all developmental stages before germination (Supplemental Fig. S2A). However, a quantitative evaluation revealed that dehiscent anthers of *exo70a2* contained a significantly higher portion of tricellular pollen grains at the expense of mature pollen grains

**Table 1.** *Segregation of the heterozygous* exo70a2 *mutant*

+/+, wild-type plants; +/−, heterozygous mutants; −/−, homozygous mutants.

| Line | Genotype | | | No. of Plants | Statistical Analysis | |
|---|---|---|---|---|---|---|
| | +/+ | +/− | −/− | *n* | $\chi^2$ | *P* |
| Expected | 25.0% | 50% | 25.0% | – | – | – |
| *exo70a2* | 38.3% | 46.7% | 15.0% | 107 | 12.14 | 0.002 |

compared to those of the wild type ($P = 0.0001$, $\chi^2$ test; Fig. 2D), indicating a defect in pollen maturation. Moreover, pollen grains from *exo70a2* homozygotes also showed significantly elevated bursting frequency in hypoosmotic conditions (wild type, 8%, $n = 477$; *exo70a2*, 14%, $n = 458$; $P < 0.0001$, $\chi^2$ test), suggesting altered exine or intine of mutant pollen grains (Supplemental Fig. S2B).

Analysis of wild-type and *exo70a2* mature pollen grains from open flowers using transmission electron microscopy revealed a higher density of endomembrane vesicles in cortical regions of *exo70a2* pollen grains compared to the wild type (*exo70a2*, 840 ± 81 vesicles•$\mu m^{-2}$ [mean ± SD], $n = 5$; wild type, 538 ± 116 vesicles $\mu m^{-2}$, $n = 5$; $P < 0.0014$, Student's *t* test), directly indicating a defect in exocytosis in *exo70a2* pollen grains (Supplemental Fig. S3)

Since high concentrations of extracellular reactive oxygen species (ROS) were reported at the onset of the pollen germination process (Smirnova et al., 2014), we analyzed ROS production in wild-type and *exo70a2* pollen grains 20 min after imbibition using histochemical staining of superoxide anion radicals by nitroblue tetrazolium (NBT). ROS levels were dramatically reduced in mutant pollen grains, indicating a different physiological status (Fig. 2, E and F).

Taken together, we conclude that *EXO70A2* is involved in pollen grain maturation, thus representing an important function assigned to the exocyst complex in plants.

### Pollen Tube Growth Is Compromised in the *exo70a2* Mutant

To determine whether the mutation affects not only pollen germination, but also pollen tube elongation, we analyzed pollen tube lengths 20 h after imbibition in vitro and found that *exo70a2* pollen tubes were dramatically shorter than wild-type ones (Figs. 2A and 3A). Subsequent analysis of growth dynamics of individual pollen tubes revealed that the average maximal growth rate of *exo70a2* pollen tubes was six times lower than that of their wild-type counterparts ($0.39 \pm 0.08$ $\mu m\ min^{-1}$ and $2.42 \pm 0.37$ $\mu m\ min^{-1}$ [mean ± SD] for *exo70a2* and the wild type, respectively; $n > 12$;, $P < 0.0001$, Student's *t* test). Interestingly, an inspection of the *exo70a2* pollen tube elongation in vivo in self-pollinated pistils showed a less dramatic, yet significant, defect in pollen tube growth compared to the wild type (Fig. 3, B and C). This can be explained by the presence of chemical signals produced by the transmitting tract tissues in pistils that promote pollen tube growth in a dose-dependent manner (Johnson and Preuss 2002; Vogler et al., 2014).

Taken together, the pollen-specific transmission defect of the *exo70a2* mutant allele is due not only to impaired pollen germination, but partly to impaired pollen tube growth. The latter defect, i.e. very short and wide pollen tubes with compromised polarity, has been previously reported for other mutants in exocyst subunits (Cole et al., 2005; Hála et al., 2008).

### Slow Growing *exo70a2* Pollen Tubes Display Morphological Defects

In the in vitro pollen germination experiments, we noticed that *exo70a2* pollen tubes had grown straight, without branching, but had an ~50% wider diameter than wild-type pollen tubes (Fig. 4, A and B). This morphological defect suggests that secretion is delocalized in the apex of *exo70a2* pollen tubes, which is consistent with the canonical exocyst function in polarized exocytosis in tip growth.

Since the exocyst plays an important role in polarized exocytosis, which in turn is crucial for cell wall construction, we tested whether the pollen tube growth defect in *exo70a2* might be due to altered cell wall biogenesis. To do so, we analyzed the distribution of dominant cell wall components in growing pollen tubes in vitro. Pectins showed normal distribution after propidium iodide staining (Fig. 4C). Callose and, especially, cellulose deposition visualized by aniline blue and calcofluor white staining, respectively, extended more toward the tip in *exo70a2* pollen tubes (Fig. 4,

**Table 2.** *Genotype analysis after reciprocal crossing of the* exo70a2 *mutant and wild type (Col-0)*

At least six independent crossings were prepared. +/+, wild-type plants; +/−, heterozygous mutants.

| Line | Pollen Recipient | Pollen Donor | No. of Plants | Statistical Analysis | | Pollen Donor | Pollen Recipient | No. of Plants | Statistical Analysis | |
|---|---|---|---|---|---|---|---|---|---|---|
| | +/+ | +/− | *n* | $\chi^2$ | *P* | +/+ | +/− | *n* | $\chi^2$ | *P* |
| Expected | 50% | 50% | – | – | – | 50% | 50% | – | – | – |
| *exo70a2* | 82.6% | 17.4% | 69 | 29.35 | <0.001 | 46.2% | 54.8% | 93 | 0.53 | 0.47 |

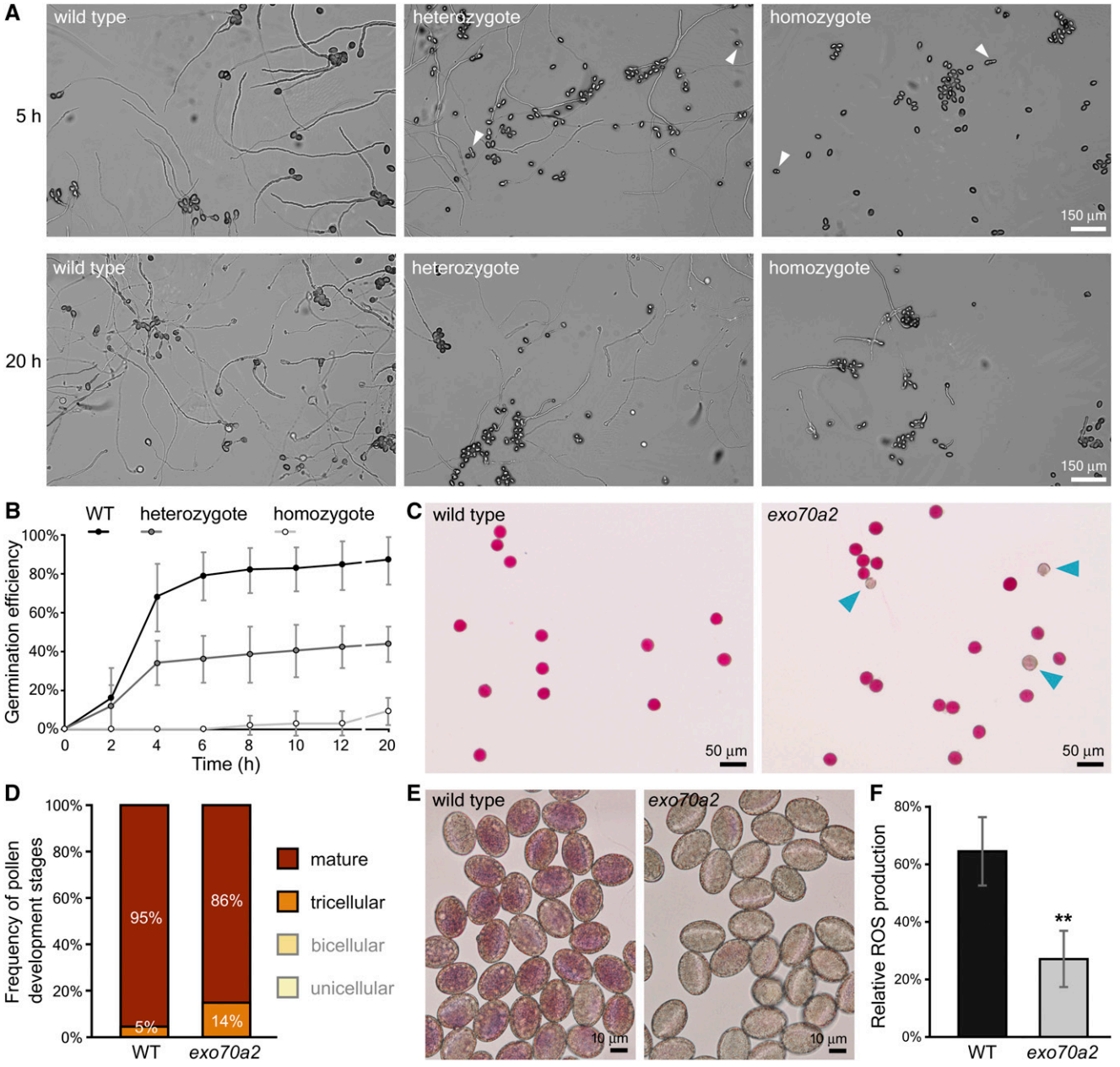


**Figure 2.** In vitro pollen germination and maturation defects of *exo70a2* mutants. A, Representative micrographs of in vitro germinated pollen from wild-type (WT) and heterozygous and homozygous *exo70a2* mutant plants 5 and 20 h after imbibition. Arrowheads indicate germinated mutant pollen tubes based on their aberrant morphology. All images are at the same scale. B, In vitro pollen germination efficiency at different time points (10 samples originating from five different plants were evaluated for each genotype; error bars represent the mean ± SD). C, Representative micrographs showing pollen viability assessed by Alexander's staining. Nonviable pollen grains are indicated by arrowheads. D, Quantification of wild-type and *exo70a2* pollen at different stages of development in open flowers ($n > 204$; $P = 0.0001$, $\chi^2$ test). Pollen was harvested from five plants of each genotype; the experiment was repeated in three biological replicates. E, ROS production 20 min after pollen imbibition as visualized by NBT staining. F, Quantification of ROS staining (in E) in wild-type and *exo70a2* pollen grains (error bars represent the mean ± SD; $n > 53$). Asterisks indicate statistical difference using Student's *t* test ($P < 0.001$). Pollen was harvested from five plants of each genotype; the experiment was repeated in three biological replicates.

D and E). This observation could be explained as a secondary effect of the much lower growth rate of mutant pollen tubes, because even wild-type pollen tubes exhibiting low growth rates, such as newly germinated or very mature pollen tubes, showed a similar cellulose deposition pattern (Supplemental Fig. S4). We

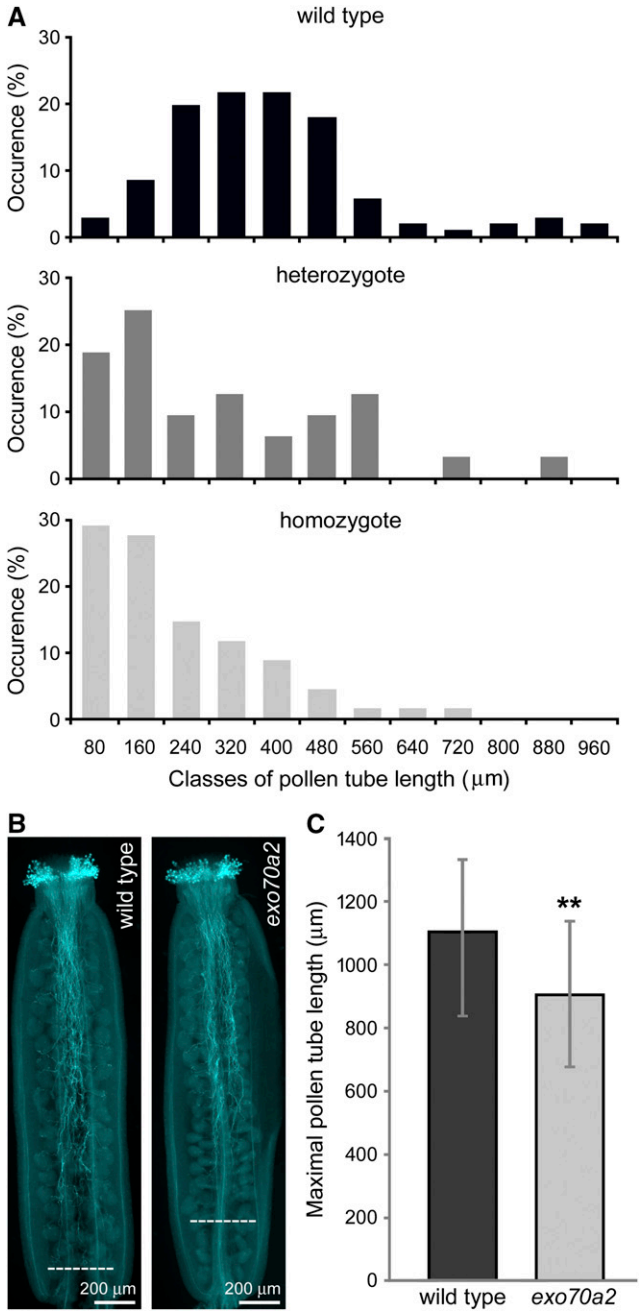


**Figure 3.** Pollen tube growth in *exo70a2* and the wild type. A, Distribution of pollen tube lengths 20 h after imbibition in vitro (related to Fig. 2A). More than 100 pollen tubes were evaluated for wild-type and heterozygous plants, and 50 pollen tubes for the *exo70a2* mutant. Pollen was collected from five different plants for each genotype, with three biological replicates. B, Aniline blue staining for visualization of callose in pollen tubes in representative self-pollinated pistils from a wild-type and a homozygous *exo70a2* plant. Dashed lines indicate the longest pollen tubes. C, Quantification of the maximal pollen tube length based on aniline blue staining. At least 30 pistils of each genotype were evaluated, with two biological replicates. Error bars represent the mean ± SD. Asterisks indicate statistical difference using Student's *t* test ($P < 0.001$).

conclude that *EXO70A2* disruption results in quantitative changes in deposition of some cell wall components in growing pollen tube tips.

### GFP:EXO70A2 Complements the *exo70A2* Mutation and Localizes to the PM in Pollen Tube Tips

For further functional characterization of EXO70A2, we prepared a GFP-tagged variant of EXO70A2 expressed under its native promoter. The *pEXO70A2::GFP:EXO70A2* construct was introduced into *exo70a2* heterozygous plants to analyze EXO70A2 localization and functionality in mutant and wild-type pollen. The expression of *pEXO70A2::GFP:EXO70A2* complemented the *EXO70A2* disruption: the percentage of nonviable pollen grains in freshly open flowers was similar to that of the wild type (complemented line, 3.9%, $n = 231$; wild type: 3.4%, $n = 179$; $P = 0.772$, $\chi^2$ test). The ability of *exo70a2* pollen to germinate in vitro without any delay was restored (Fig. 5, A and B; Supplemental Fig. S5), the pollen tube growth defect was reverted to normal (Fig. 5C), and the pollen tube width was similar to wild-type tubes (6.20 ± 0.45 µm 6.37 ± 0.71 µm for the complemented line and the wild type, respectively [mean ± SD]; $n = 32$; $P = 0.257$, Student's *t* test). These observations confirm that the reported defects in the *exo70a2* pollen were due to the disruption of the *EXO70A2* gene.

While seedlings and mature sporophytic organs exhibited no fluorescence signal attributed to GFP:EXO70A2 (not shown), we clearly detected GFP:EXO70A2 in pollen grains and pollen tube tips (Fig. 6). GFP:EXO70A2 was localized mostly in the nucleolus in unicellular pollen and in both vegetative- and generative-cell nuclei in bicellular pollen. In tricellular pollen, it strongly accumulated in the whole cytoplasm up to the PM and periphery of the vegetative nucleus, with some remnants inside the nucleus, and in mature pollen grains, it was weakly present in the cytoplasm, enriched around the vegetative-cell nucleus and sperm cells, but excluded from the lumen of all nuclei (Fig. 6A). The obviously higher signal intensity of GFP:EXO70A2 at the tricellular stage corresponds to the maximum level of EXO70A2 mRNA expression across pollen developmental stages based on microarray data (Synek et al., 2017). Importantly, in complemented *exo70a2* pollen tubes, GFP:EXO70A2 displayed a highly polarized localization along the PM in the apical domain of growing pollen tube tips, with a minor portion in the cytoplasm (Fig. 6B), which is a typical localization pattern for exocyst subunits in pollen tubes (Hála et al., 2008; Synek et al., 2017). In the wild-type background, however, the polar PM localization was absent and GFP:EXO70A2 was distributed entirely in the cytoplasm of pollen tubes (Fig. 6C), which could be explained by a competition of the native and GFP-tagged EXO70A2 variants for binding to the exocyst complex, as observed previously in tobacco (*Nicotiana*

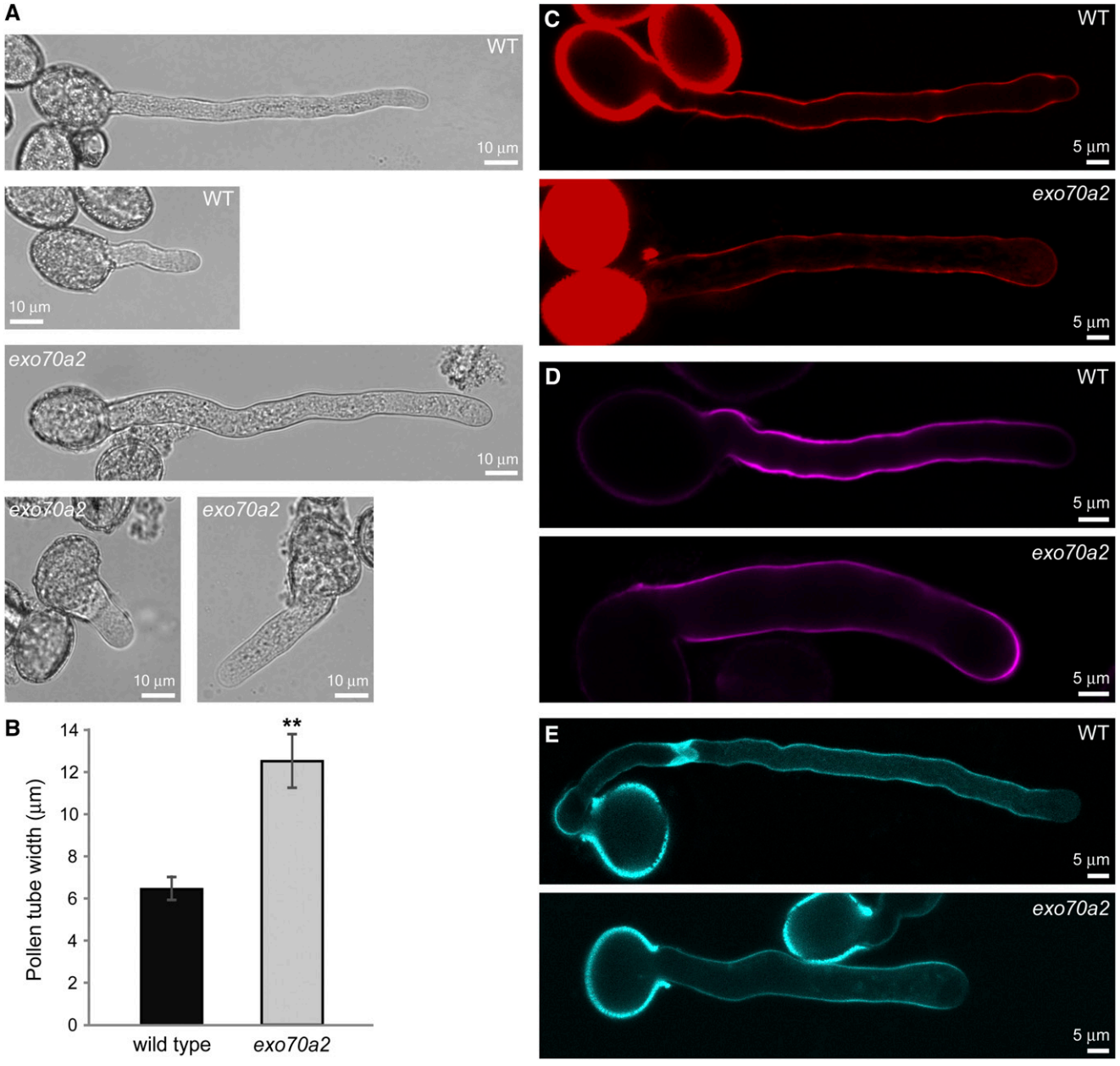


**Figure 4.** Morphology and cell wall deposition of *exo70a2* and wild-type pollen tubes grown in vitro. A, Wild-type (WT) and *exo70a2* pollen tubes 1.5 and 8 h after imbibition. B, Measurement of wild-type and *exo70a2* pollen tube width (error bars represent the mean ± SD; $n = 40$). Asterisks indicate statistical difference using Student's *t* test ($P < 0.001$). Pollen was collected from five different plants for each genotype, with two biological replicates. C to E, Visualization of pectins by propidium iodide staining (C), cellulose by Calcofluor White staining (D), and callose by aniline blue staining (E).

*tabacum*) pollen tubes (Sekereš et al., 2017), and also in mammalian cells (Matern et al., 2001).

### EXO70A2 Can Rescue the *exo70a1* Mutation in the Sporophyte

Next, we were interested in the degree of functional specialization versus redundancy of EXO70A1 and EXO70A2 paralogs. In order to address this question experimentally, we expressed *EXO70A2* and *EXO70A1*, respectively, under control of the *EXO70A1* promoter in the *exo70a1* mutant background and compared their localization and functionality in the sporophyte. The *exo70a1* mutant was earlier shown to exhibit pleiotropic morphological defects, including retarded polar growth of root hairs, loss of apical dominance, dwarfish stature, and sterility (Synek et al., 2006). Moreover, GFP:EXO70A1 fully complemented the *exo70a1* loss-of-function allele and localized at the PM,

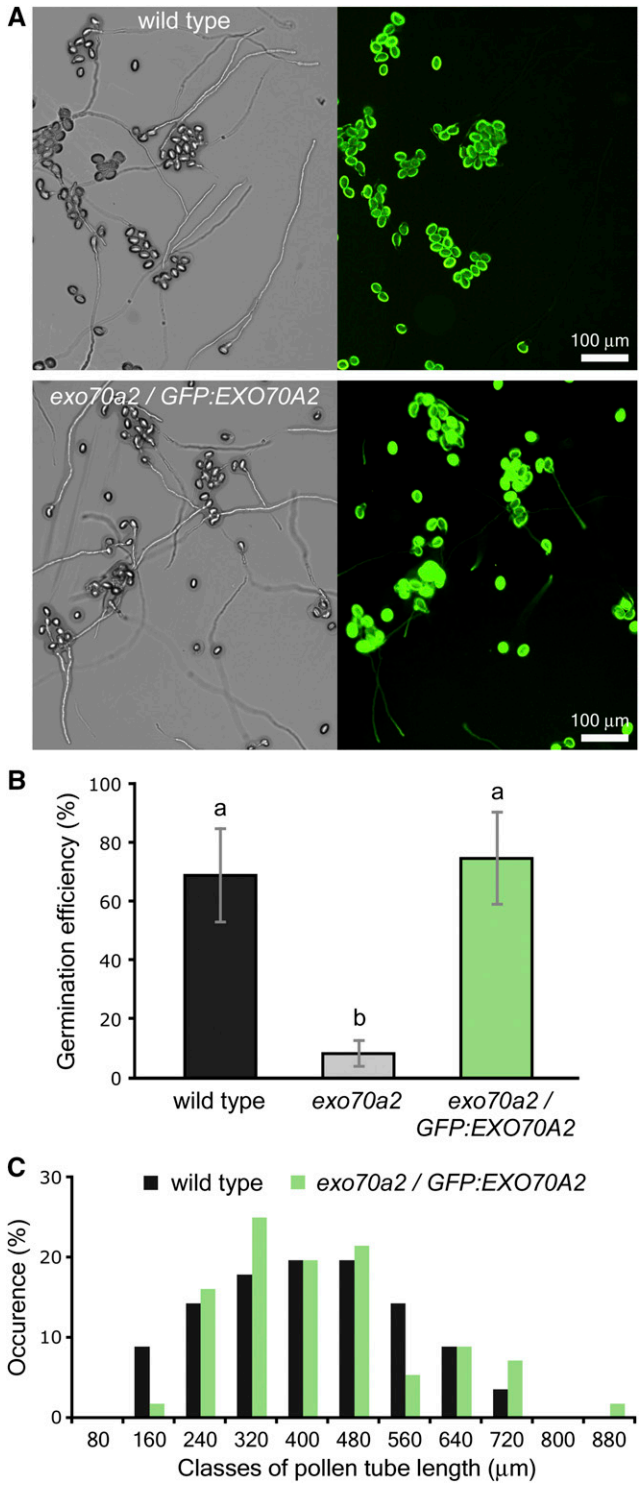


**Figure 5.** Expression of *pEXO70A2:: GFP:EXO70A2* complements defects of the *exo70a2* mutant pollen. A, Representative micrographs of in vitro germinated pollen from the wild type and the *exo70a2/pEXO70A2::GFP:EXO70A2* line 20 h after imbibition. Bright-field images are shown at left and green fluorescence images at right. B, Pollen germination efficiency 20 h after imbibition in vitro. Error bars represent the mean ± SD ($n > 145$). Lowercase letters denote statistically significant different groups evaluated by ANOVA ($P < 0.01$). C, Distribution of pollen tube lengths 20 h after imbibition ($n > 60$). Ten samples originating from five different plants were evaluated for each genotype, with two biological replicates.

with special enrichment at the outer lateral domain in root epidermal cells (Drdová et al., 2013; Fendrych et al., 2013).

We found that the expression of *pEXO70A1::GFP:EXO70A2* rescued the morphological defects of *exo70a1* mutant plants similarly to *pEXO70A1::GFP:EXO70A1*, as demonstrated by measurements of plant height and overall morphology (Fig. 7, A and B). Importantly, the subcellular localization of GFP:EXO70A2 in root epidermal cells was indistinguishable from that of GFP:EXO70A1 (Fig. 7C). We conclude that EXO70A1 and EXO70A2 paralogs have a potential to be functionally redundant in the sporophyte.

Furthermore, the EXO70A2 disruption had an additive effect on the disruption of EXO70A1. In contrast to small *exo70a1* mutants, seedlings of the *exo70a1 exo70a2* double mutant were even smaller short-living dwarf plants that exhibited significantly shorter roots and shoots, characterized by asymmetric, reduced, or completely missing cotyledons (Fig. 7, D and E; Supplemental Fig. S6). Subsequent analysis of *EXO70A2* expression in wild-type, *exo70a1*, and *exo70a2* seedlings using RT-sqPCR revealed that *EXO70A2* is weakly expressed in the sporophyte and its expression is upregulated in the *exo70a1* knockout when compared to wild-type seedlings (Supplemental Fig. S7). The PCR product was sequenced to prove its *EXO70A2* identity. Collectively, the comparison of single- and double-mutant phenotypes and the detection of *EXO70A2* in seedlings suggest that EXO70A2 is expressed even in the sporophyte, in addition to its dominant role in the male gametophyte, and is able to partly substitute for the EXO70A1 function.

### EXO70A1 Cannot Substitute for EXO70A2 in the Pollen

In parallel with the previous experiment, we tested whether EXO70A1 could provide a similar function to EXO70A2 in pollen when ectopically expressed under the control of the *EXO70A2* promoter in the *exo70a2* background. *pEXO70A2::*GFP:EXO70A1 was detected in a pattern similar to that observed for *pEXO70A2::*GFP:EXO70A2 in *exo70a2* pollen grains (Fig. 8A). However, pollen of these transgenic plants was unable to germinate, although we analyzed six plants originating from two independent transformations done using the same cloning strategy and materials as for the previous constructs (Fig. 8B). We conclude that when EXO70A2 is disrupted, EXO70A1 cannot substitute for its function in pollen, despite the functional redundancy of these two isoforms observed in the sporophyte.

To explain this discrepancy, we compared structural models of EXO70A1 and EXO70A2 based on

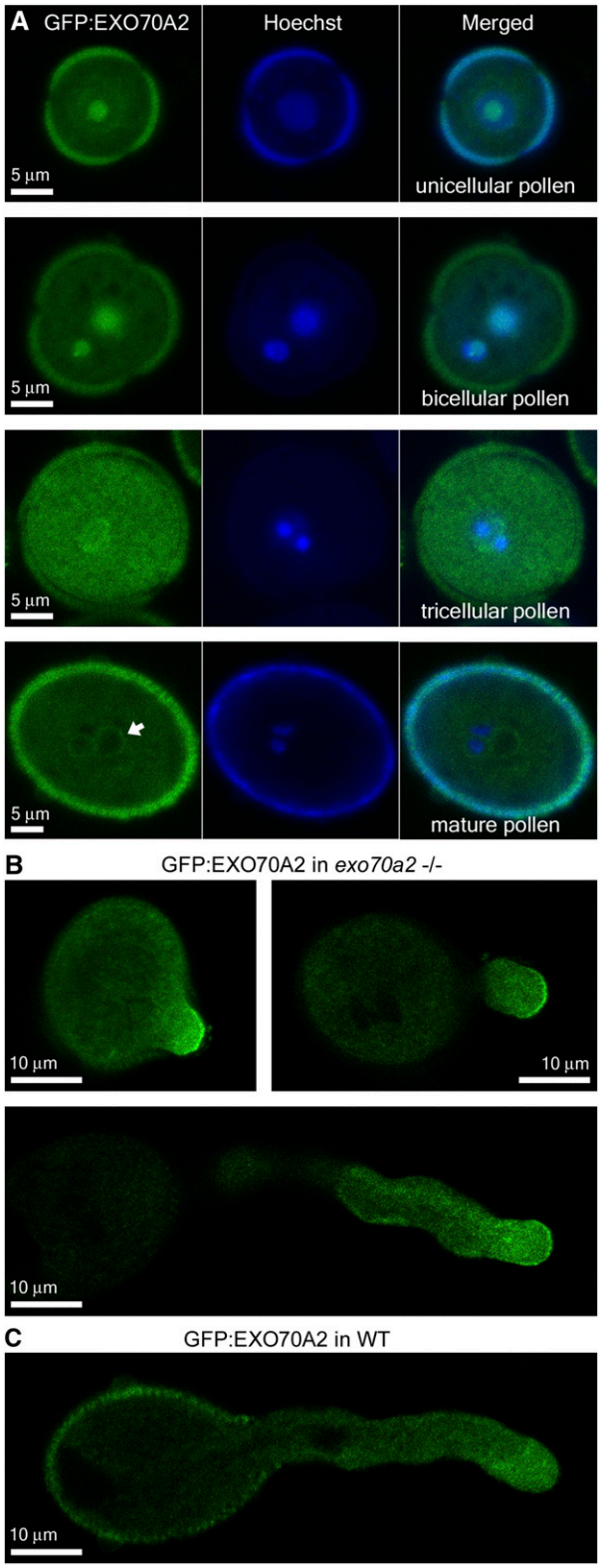


**Figure 6.** Localization of GFP:EXO70A2 expressed under its native promoter in pollen. A, GFP:EXO70A2 localization in unicellular, bicellular, tricellular, and mature pollen grains in the *exo70a2* background. All images were captured at the same setting, allowing for relative quantitative comparison. B, GFP:EXO70A2 localization at different stages of pollen tube elongation in the *exo70a2* background. C, GFP:EXO70A2 localization in a pollen tube in the wild-type (WT) background.

crystallographic data generated from yeast (*Saccharomyces cerevisiae*) Exo70 and Arabidopsis EXO70A1 (Dong et al., 2005; Hamburger et al., 2006; Zhang et al., 2016; Pleskot et al., 2015; Mei et al., 2018). We noticed substantial differences in the amino acid composition in a medial plant-specific loop and on the side of the EXO70A2 molecule facing out of the PM (Supplemental Fig. S8). The variability was manifested by a different electrostatic potential on the EXO70A2 surface in the loop and C terminus. This analysis suggests that EXO70A1 versus EXO70A2 may interact with specific proteins in the sporophyte or male gametophyte, respectively, that modulate their function.

## DISCUSSION

Proper pollen development, efficient pollen germination, and pollen tube growth are essential processes for successful plant fertilization. These processes include cell expansion and cell wall maturation, which require highly efficient secretory machinery, delivering cell wall components and PM-associated materials to specific sites at the PM. To sustain such demands, polarized secretion is regulated by a number of molecular regulators, including the vesicle-tethering exocyst complex. The crucial role of several core exocyst subunits in pollen germination and pollen tube tip growth was previously described (Cole et al., 2005; Hála et al., 2008; Bloch et al., 2016). However, the main EXO70 isoform contributing to the conventional secretory function of the exocyst complex in pollen has not been characterized until now.

We previously described how EXO70.2 clade members EXO70C2 and EXO70C1 are not stable subunits of the exocyst complex (Synek et al., 2017), leaving EXO70A2 as the best candidate for the main housekeeping EXO70 isoform in pollen. First, EXO70A2 is the closest paralog to EXO70A1—the main EXO70 isoform in the Arabidopsis sporophyte—and the two share 72% sequence identity at the protein level. Second, similar to EXO70A1, EXO70A2 physically interacted with three other exocyst subunits (SEC3a, SEC10b, and EXO84b; Hála et al., 2008; Fendrych et al., 2010; Synek et al., 2017). Third, the expression patterns of *EXO70A1* is sporophyte specific, whereas that of *EXO70A2* is pollen specific. This is in agreement with the hypothesis that after whole-genome duplication in plants, genes directly linked to cell polarity tend to diverge in expression pattern to sporophyte specific and to those enriched in tip-growing cells, especially in the male gametophyte (De Smet et al., 2017). In general, about 10% to 40% of Arabidopsis genes are selectively expressed in pollen, and these genes are enriched in signaling, vesicle trafficking, the cytoskeleton, and

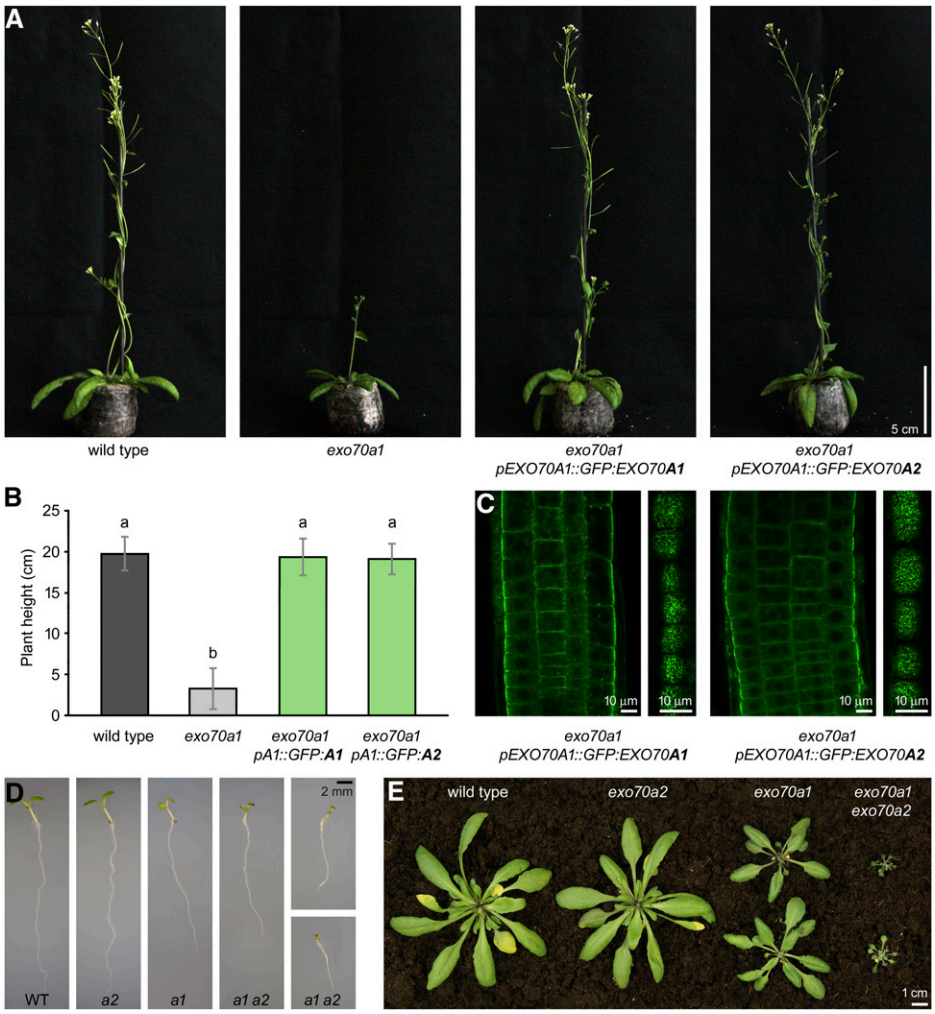


**Figure 7.** Ectopic expression of EXO70A2 in sporophytic tissues of *exo70a1* mutant plants. A, Representative images of 6-week-old plants expressing *pEXO70A1::GFP:EXO70A1* or *pEXO70A1::GFP:EXO70A2* in the *exo70a1* background in comparison to wild-type (WT) and *exo70a1* plants. All images are at the same scale. B, Measurement of 6-week-old plant height. At least 22 plants were evaluated for each genotype, with two biological replicates. Bars represent the mean ± SD. Lowercase letters denote statistically significant different groups evaluated by ANOVA ($P < 0.01$). C, Localization of *pEXO70A1::GFP:EXO70A1* or *pEXO70A1::GFP:EXO70A2* in root epidermal cells. Confocal sections through the root transition zone (left) and at the level of lateral PMs (right) are shown. D, Representative images of 1-week-old seedlings grown in vitro, showing additive defects in *exo70a1 exo70a2* double mutants. All images are at the same scale. E, Representative images of 4-week-old plants, showing additive defects in *exo70a1 exo70a2* double mutants.

membrane transport (Becker et al., 2003; Honys and Twell, 2003). Importantly, EXO70A2 still retains the capacity to function as an exocyst subunit in sporophytic cells, whereas EXO70A1 is unable to substitute for EXO70A2 function in pollen, possibly due to its inability to bind EXO70A2-specific protein interactors in the male gametophyte.

In the course of the extraordinary diversification and functional specialization of the large EXO70 family in angiosperms (Cvrčková et al., 2012), the EXO70A duplication to sporophyte- and male gametophyte-specific paralogs occurred independently in monocots and eudicots. In some plant taxonomic groups, each further duplicated, generating, for example, EXO70A2 and EXO70A3 in Brassicaceae (Cvrčková et al., 2012). An analogous situation, i.e. the presence of pollen-expressed and sporophyte-expressed paralogs, has been documented in the case of SEC3, SEC15, and EXO84 exocyst subunits in Arabidopsis (Bloch et al., 2016; Synek et al., 2017; K. Batystová, M. Klejchová, E. Janková Drdová, L. Synek, P. Sabol, M. Potocký, V. Žárský, and M. Hála, unpublished data). Analagous to our observation that artificial EXO70A2 expression in the sporophyte could complement the sporophytic defects of *exo70a1* mutants, SEC15a, the main SEC15 isoform in Arabidopsis pollen, could substitute for the function of SEC15b in the sporophyte, although SEC15a and SEC15b share a mere 47% sequence identity at the protein level (K. Batystová, M. Klejchová, E. Janková Drdová, L. Synek, P. Sabol, M. Potocký, V. Žárský and M. Hála, unpublished data). In contrast, Arabidopsis SEC10a and SEC10b represent a very recent duplication, with no diversification in their expression or function (Vukašinović et al., 2014).

Based on the phenotypic differences observed in *exo70a2* mutants, we documented that EXO70A2 participates in pollen maturation, germination, and pollen tube growth. In line with this, other recently reported *exo70a2* point mutation alleles show defects in germination efficiency and pollen tube growth (Beuder et al., 2020). However, in contrast to that report, our data imply that the primary defect in *exo70a2* mutants may be related to its function in pollen maturation and that the germination defect might in fact be a combination of both compromised pollen maturation and impaired tip targeting of the exocytosis pathway. Similarly, mutants in two other exocyst subunits, *sec3a* and *sec8*, also exhibited severe defects in germination efficiency (Cole

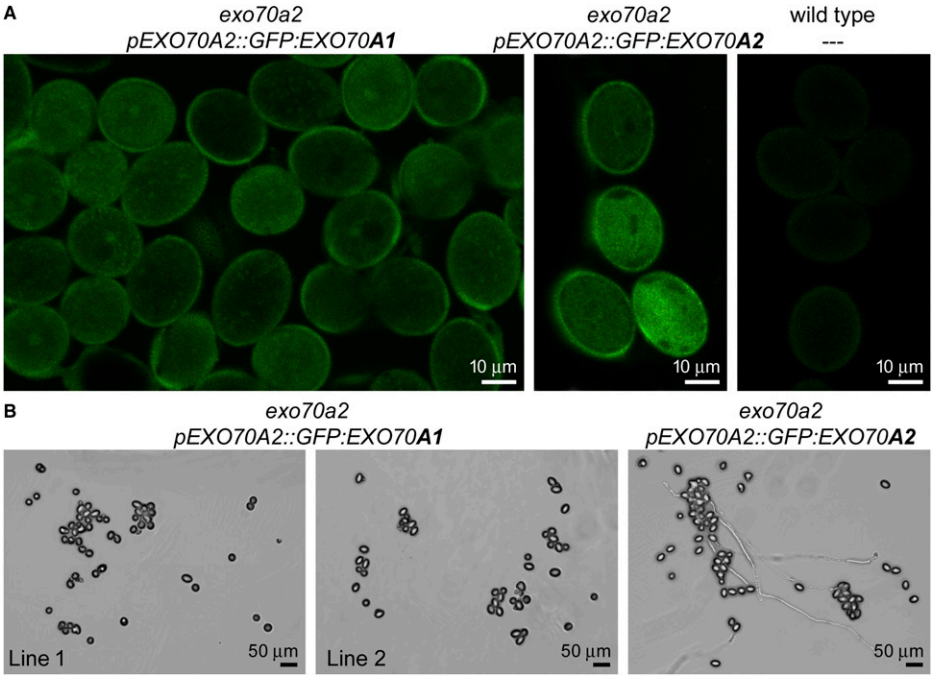


**Figure 8.** Ectopic expression of EXO70A1 in the pollen of *exo70a2* mutant plants. A, Localization of *pEXO70A2::GFP:EXO70A1* in the pollen from open flowers in comparison to positive (*pEXO70A2::GFP:EXO70A2*) and negative (wild-type) controls. B, Representative micrographs of in vitro germinated pollen from plants expressing *pEXO70A2::GFP:EXO70A1* (two independent lines) or *pEXO70A2::GFP:EXO70A2* in the *exo70a2* mutant background 20 h after imbibition.

et al., 2005; Bloch et al., 2016). A higher percentage of nonviable and bursting pollen grains and delayed germination in *exo70a2* could be explained by mislocalization or inefficient delivery of some cell wall-modifying enzymes (or cell wall components) whose trafficking during pollen maturation and germination depends on the EXO70A2-containing exocyst complex. Indeed, we observed accumulation of endomembrane vesicles in cortical regions of *exo70a2* pollen grains. In agreement, it has been documented that proper structure and chemical characteristics of the cell wall are essential for efficient pollen germination and pollen tube growth (Chebli et al., 2012; Leroux et al., 2015; MacAlister et al., 2016). For example, the Arabidopsis mutant in pollen-specific pectin methylesterase (PME48) showed delayed pollen grain germination and bursting of pollen tubes (Leroux et al., 2015). Likewise, triple and quadruple mutants in pollen-expressed Leu-rich repeat extensins (LRX8–LRX11) showed a high proportion of ungerminated and burst pollen grains and defective pollen tubes (Wang et al., 2018). Also, the reduction of pectic arabinan side chains, caused by ectopic expression of endo-$\alpha$-1,5-L-arabinanase (eGARA), resulted in collapsed pollen grains with altered intine during pollen maturation in potato (*Solanum tuberosum*; Cankar et al., 2014).

One of the crucial regulatory modules in pollen germination and pollen tube growth is ROS production (Potocký et al., 2007, 2012; Smirnova et al., 2014). Two Arabidopsis pollen-specific NADPH oxidases localized at the PM, RBOHH and RBOHJ, were necessary for ROS accumulation in the pollen grain cell wall upon pollination and later in pollen tube tips. Double mutants in these genes exhibited a much lower level of ROS, resulting in collapsing pollen tubes (Lassig et al., 2014; Kaya et al., 2015). Interestingly, data of Smirnova et al. (2014) suggest that targeted production of extracellular ROS is required for changes in mechanical properties of the intine in pollen grains underlying efficient germination. Since we observed a significant decrease in ROS production in *exo70a2* germinating pollen grains, we suggest that the pollen exocyst may function in the delivery of NADPH oxidases to specific sites at the PM during germination.

Following pollen germination, rapidly elongating pollen tubes require precisely regulated secretory machinery to support their intensive tip growth. Similar to *exo70a2* in this study, mutants in several core exocyst subunits (*sec5a/b*, *sec6*, *sec8*, and *sec15a*) generate extremely short and wide pollen tubes with drastically reduced fertilization capacity (Hála et al., 2008). Reduced transmission efficiency and pollen tube elongation of *exo70a2* mutants were observed also by Beuder et al. (2020). The pollen tube phenotype is most likely caused by an inefficient targeting of secretory vesicles, possibly carrying some specific cargo, to the growing tip. For example, mutants in Hyp O-arabinosyltransferases HPAT1 and HPAT3, involved in modification of cell wall-associated extensins (MacAlister et al., 2016), and pectin methylesterases PPME1 (Tian et al., 2006) and VANGUARD1 (Jiang et al., 2005) exhibited a pollen tube elongation defect similar to that observed in *exo70a2*. Cell wall and pollen tube morphology defects of the *hpat1 hpat3* double mutant were partly suppressed by disruption of *EXO70A2*, and also *SEC15a*, further indicating the involvement of EXO70A2 and possibly the whole exocyst complex, in targeted secretion in growing pollen tube tips (Beuder et al., 2020). However, our data clearly show that the EXO70A2 function is essential for efficient pollen maturation.

The PM localization of EXO70A2 in growing pollen tube tips (also observed in Beuder et al., 2020) was identical to that of core exocyst subunits SEC8, SEC10a, and SEC15a (Synek et al., 2017; K. Batystová, M. Klejchová, E. Janková Drdová, L. Synek, P. Sabol, M. Potocký, V. Žárský and M. Hála, unpublished data). At the molecular level, EXO70A2 likely mediates the exocyst interaction with the PM, similar to Exo70 in yeast and mammalian cells (Boyd et al., 2004; He et al., 2007; Pleskot et al., 2015). This notion is supported by the observation that the N-terminally truncated SEC3a subunit in Arabidopsis pollen was unable to interact with the PM but still localized to the apical PM in growing pollen tube tips as a part of the complex (Bloch et al., 2016). However, SEC3, known to mediate interaction of the Arabidopsis exocyst with active ROP GTPases via the ICR1 adaptor protein (Lavy et al., 2007), might perhaps be at least partly functionally redundant in exocyst PM targeting with the EXO70A2 function. ROP GTPases and their regulators (such as the REN1 GAP) are known to be localized at the pollen tube tip, similar to EXO70A2, and are crucial for cell polarity establishment and maintenance (Hwang et al., 2008; Li et al., 2008).

Although the transmission efficiency of the *exo70a2* mutant allele was heavily impaired, it was not as strong as in loss-of-function mutants (*sec6*, *sec8*, and *sec15a*) in the core exocyst subunits (Hála et al., 2008). This indicates that some other EXO70 isoform(s) could provide a function partially overlapping with that of EXO70A2, with possible candidates including EXO70H3, EXO70H5, and EXO70H6. However, the abundance of these isoforms in the pollen proteome is most likely very low (Synek et al., 2017), and their relevance thus would have to be proved experimentally. Alternatively, *EXO70A1* might be activated when *EXO70A2* is disrupted, despite the fact that *EXO70A1* is normally not expressed in pollen (www.Genevestigator.com; Hruz et al., 2008; Grobei et al., 2009). We propose that the other six EXO70 isoforms expressed in pollen adopted specific functions showing no or only partial functional overlap with that of EXO70A2. In addition, their activities might be restricted to certain stages of pollen development or specific endomembrane domains.

In summary, we conclude that among seven EXO70 isoforms expressed in the Arabidopsis male gametophyte, EXO70A2 is the main isoform, contributing to the conventional exocyst function in exocytosis, like its sibling, EXO70A1, in the sporophyte. However, EXO70A2 is important not only for pollen germination and highly polarized pollen tube growth, but also for pollen grain maturation. This indicates that the exocyst plays a role in functional continuity between pollen maturation and the following processes, pollen germination and pollen tube growth. Despite the deep evolutionary split in eudicots, EXO70A2 still retains the ability to fully substitute for the EXO70A1 function in the sporophyte, whereas EXO70A1 lost the capacity to function in pollen development. The duplication of *EXO70A* genes to sporophyte- and male gametophyte-specific paralogs occurred independently in monocots and eudicots, suggesting convergent functional evolution of pollen-specific versions of the exocyst complex in angiosperms—an interesting challenge for future explorations.

## MATERIALS AND METHODS

### Phylogenetic and Expression Analysis

To perform the phylogenetic analysis, a set of EXO70.1 clade sequences from our previous studies (Cvrčková et al., 2012; Rawat et al., 2017) has been updated according to their newest database status, and homologs from additional plant species were obtained by BLASTP searches of the GenBank, Phytozome (Goodstein et al., 2012), and GDR (www.rosaceae.org) databases using Arabidopsis (*Arabidopsis thaliana*) EXO70A1 (At5g03540) and EXO70A2 (At5g52340) sequences as a query. The full list of sequences is provided in Supplemental File S1. Protein sequence alignment was constructed using the MAFFT E-INS-I algorithm (Katoh and Standley, 2013) in Jalview software (Waterhouse et al., 2009). Gaps and nonconserved regions were then manually deleted from the alignment, giving a matrix of 56 taxa and 546 positions. Bayesian phylogeny inference was performed using MrBayes software (Ronquist et al., 2012) with a WAG amino acid model, where the analysis was performed in four runs with four chains and 500,000 generations, and trees were sampled every 100 generations. All four runs asymptotically approached the same stationarity after the first 125,000 generations, which were omitted from the final analysis. Maximum-likelihood phylogeny was performed in Phyml software (Guindon et al., 2010) using the LG matrix $\gamma$-corrected for among-site rate variation with four rate site categories plus a category for invariable sites, with all parameters estimated from the data model to build the phylogenetic tree. Bootstrap analysis (500 replicates) was performed to estimate the probability of maximum-likelihood tree topology.

Analysis of the EXO70.1 paralog expression in male gametophytic and sporophytic tissues was performed using the CoNekT (Proost and Mutwil, 2018) and GEO (Barrett et al., 2013) tools. Transcript abundance of tobacco EXO70.1 isoforms in pollen was assessed by reanalyzing RNA-sequencing data generated by Conze et al. (2017) according to Ghosh and Chan (2016). We used transcripts per kilobase million-based normalization, because it could be used for gene count comparisons both within a sample and between samples of the same sample group (Abrams et al., 2019). Briefly, raw data reads were analyzed using fastQC and mapped to a reference gene-set (TN90 cultivar) using tophat. Cufflinks was used to assemble and reconstruct the transcriptome and calculate transcripts per kilobase million expression values. Additional anther/pollen RNA-sequencing data for sorghum (*Sorghum bicolor*), Arabidopsis, poplar (*Populus* spp.), strawberry (*Fragaria* spp.), and pear (*Pyrus* spp.) were obtained from Davidson et al. (2012), Loraine et al. (2013), Zhao et al. (2016), Zhou et al. (2016), and Hollender et al. (2014), respectively.

### Plant Material and Growth Conditions

The Arabidopsis *exo70a1-2* (SALK_135462; Synek et al., 2006) and *exo70a2-1* (GABI_824D06; Synek et al., 2017) lines were described previously. The *exo70a2* line FLAG_264F01 was obtained from the Institut National de la Recherche Agronomique. Genotypes of individual plants were always analyzed by PCR genotyping (for primers, see Supplemental Table S1). To prepare the *exo70a1 exo70a2* double mutant, *exo70a1-2* was crossed to CRISPR-generated *exo70a2-4*.

Seeds were surface sterilized (70% [v/v] ethanol for 3 min and 20% [v/v] commercial bleach for 5 min), rinsed four times with sterile distilled water, and stratified for 2 d at 4°C. Seeds were germinated on vertical agar plates (one-half strength Murashige and Skoog [Duchefa Biochemie] supplemented with 1% [w/v] Suc, vitamin mixture, and 1% [w/v] plant agar [Duchefa Biochemie]) at 22°C under long-day conditions (16 h light/8 h dark). Seedlings were transferred to turf pellets (Jiffy Products International) after 8 d and grown until harvest at the same growth conditions.

### Preparation of the *exo70a2* Mutant Line

The new Arabidopsis mutant line (*exo70a2-4*) was generated using egg cell-specific promoter-controlled CRISPR/Cas9 technology, employing the pHSE401E vector (Wang et al., 2015). To increase the chance of a mutation, two

target single-guide RNAs were designed. Sequences of the CRISPR target sites were carefully checked by BLAST against all other EXO70 paralogs in the Arabidopsis genome to exclude unintended targeting of additional EXO70 paralogs (target site 1, AGCTAAAATATTGAG; target site 2, GGATACTCGAGCTG). Flowering Arabidopsis plants of the Columbia-0 ecotype (NASC collection) were transformed using the *Agrobacterium tumefaciens*-mediated floral dip method (Clough and Bent, 1998). After selection on hygromycin, mutant lines were identified by sequencing of PCR products obtained from the targeted part of the *EXO70A2* gene (At5g52340). A mutant line having a 13-bp insertion in the expected site (...TCGAGCTGCGGTttcatgcgatttttGTTGGAACAGAG...), causing a premature stop codon due to a frameshift, was further characterized. The genotype was then routinely analyzed by PCR genotyping, where two primers, one from each pair for the wild type and mutant allele, were designed over the CRISPR-modified site (Supplemental Fig. S1A; Supplemental Table S1).

## Semiquantitative RT-PCR Analysis of the *EXO70A2* Transcription

To determine the *EXO70A2* transcript level in the CRISPR-modified mutant line, total RNA was extracted from 100 mg of apical parts of primary inflorescences of *exo70a2* and wild-type plants using the RNeasy kit (Qiagen). Prior to reverse transcription, samples were treated by DNase I (New England Biolabs). The complementary DNA (cDNA) was synthesized using 2 $\mu$g of total RNA, oligo(dT) primers and Transcriptor High Fidelity cDNA Synthesis kit (Roche). Transcript abundance was assayed by RT-sqPCR for two gene regions, upstream and downstream from the CRISPR-generated insertion (see Supplemental Fig. S1), using *EXO70A2*-specific primers (Supplemental Table S1); the primers were checked for potential interference with *EXO70A1* and *EXO70A3* paralogs. ACTIN7-specific primers were used as a quantitative control (Supplemental Table S1). The optimal number of PCR cycles was determined empirically.

For determination of the *EXO70A2* transcript level in the sporophyte, the procedure was similar, with the following differences: total RNA was extracted from 100 mg of 20-d-old seedlings of the wild type, *exo70a1*, and *exo70a2*. Primers were specific for the downstream part of the *EXO70A2* cDNA (Supplemental Table S1).

## Analysis of Pollen Development

Pollen grains at different developmental stages were collected from a series of flower buds ending with a freshly opened flower and used for further analyses of pollen grain viability, maturation, and nuclear composition.

To inspect pollen grain viability, we used Alexander staining (Alexander, 1969) with the following modifications: 10× dilution, 15 min incubation time at room temperature. Images were captured using a Nikon Eclipse 90i microscope with Plan Apo 10×/0.45 objective, differential interference contrast (DIC) optics, and a Zyla sCMOS camera (Andor). Fully developed viable and nonviable pollen grains were scored. Underdeveloped collapsed grains were excluded from the analysis.

To analyze the nuclear composition, pollen grains were stained with 4′,6-diamino-2-phenylindole at a final concentration of 4 $\mu$g mL$^{-1}$ in pollen isolation buffer (100 mM $Na_3PO_4$ [pH 7.5]; 1 mM EDTA; and 0.1% [v/v] Triton X-100) as described by Backues et al. (2010). Images were captured using a Zeiss Axio Imager 2 microscope with an EC Plan-Neofluar 40×/0.75 objective, a filter set for observation of blue fluorescence, DIC optics, and a Zeiss Axiocam 506 Color camera.

For analysis of the nuclear composition, pollen grains expressing *GFP:EXO70A2* were stained with Hoechst 33258 at a final concentration of 1 mg mL$^{-1}$ in liquid pollen germination medium. After 30 min, pollen grains were imaged using a Zeiss LSM 880 confocal laser scanning microscope with Plan-Apochromat 40×/1.2 WI objective.

Pollen from 10 open flowers was harvested from five plants per genotype and extracted in 1 mL of fresh liquid pollen germination medium by three times repeated vortexing and centrifugation steps (1 min vortexing, 3 min centrifugation at 3,000 rpm). Pollen pellets were resuspended in 15 $\mu$L of Ruthenium red solution in distilled water (final concentration 0.14 mg mL$^{-1}$). Images were taken using a Nikon Eclipse 90i microscope with Plan Apo 4×/0.2 and Plan Apo 10×/0.45 objectives.

## Transmission Electron Microscopy

For transmission electron microscopy, pollen suspensions from open flowers of the wild type and *exo70a2* were fixed for 24 h in 2.5% (v/v) glutaraldehyde in 0.1 M cacodylate buffer (pH 7.2) and postfixed in 2% (w/v) $OsO_4$ in the same buffer. Samples were then dehydrated through an ascending ethanol and acetone series and embedded in Araldite-Poly/Bed 812 mixture. Thin sections (70 nm) were cut on a Reichert-Jung Ultracut E ultramicrotome and stained using uranyl acetate and lead citrate. Sections were examined and photographed using a JEOL JEM-1011 electron microscope.

## Germination of Arabidopsis Pollen In Vitro

Pollen was germinated on a thin layer of semisolid pollen germination medium (10% [w/v] Suc, 1.5% [w/v] low-melting-point agarose [Agarose-Universal, peqGOLD, VWR], 0.01% [w/v] $H_3BO_3$, 5 mM $CaCl_2$, 5 mM KCl, and 1 mM $MgSO_4$) in a chambered Lab-Tek II coverglass (Thermo Scientific). Pollen grains from fully opened flowers were spread onto the medium layer and chambers were closed and placed into standard plant growth conditions (see above).

To evaluate germination efficiency, pollen grains were scored as germinated when a pollen tube length reached at least one-half of the pollen grain diameter. For each genotype, 10 samples originating from five different plants were observed. Pictures of germinated pollen were taken using a Nikon Eclipse 90i microscope with a Plan Apo 10×/0.45 objective. Pollen tube lengths were measured in ImageJ and histograms were generated in Microsoft Excel.

## ROS Staining

Production of superoxide was determined by its ability to reduce NBT to formazan precipitate (Rossetti and Bonatti, 2001). Pollen grains were spread on semisolid pollen germination medium (see above). After 20 min of imbibition, they were overlaid with 20-$\mu$L drops of NBT diluted in liquid pollen germination medium to a final concentration 2 mg mL$^{-1}$, incubated for 10 min, and immediately imaged using a Nikon Eclipse 90i microscope with a Plan Apo 20×/0.75 objective, excluding DIC filters, and maximum field aperture opening. NBT signal intensity was measured in ImageJ. Values were normalized to that of nonstained pollen grains and related to maximal staining intensity value across all samples. The experiment was repeated in three replicas with similar results.

## Pollen Tube Morphology and Growth Rate

Details of pollen tube morphology were captured using a Zeiss Axio Imager 2 microscope with an EC Plan-Neofluar 40×/0.75 objective at 3 and 16 h after imbibition for the wild type and *exo70a2*, respectively. The pollen tube growth rate was analyzed using the same microscope but with an EC Plan-Neofluar 20×/0.5 objective. Time-lapse photographs at 2-min intervals were recorded for 30 min for the wild type (starting 3 h after imbibition) and 90 min for *exo70a2* (starting 16 h after imbibition). Only pollen tubes longer than twice the pollen grain diameter were evaluated, because they already had reached the maximal growth rate.

## Callose Visualization in Arabidopsis Pistils

Self-pollinated pistils (at least 30 for each genotype) from fully opened flowers were collected and stained with aniline blue according to Mori et al. (2006) and imaged using a Nikon Eclipse 90i microscope with a Plan Apo 4×/0.2 objective and a Zyla sCMOS camera (Andor). Length of the longest pollen tube in every pistil was measured, and recorded values were evaluated statistically using Student's *t* test.

## Fluorescent Staining of Cell Wall Components

Propidium iodide, Calcofluor White, or Aniline Blue was diluted in liquid germination medium and gently applied onto pollen germinated in vitro immediately before imaging. Images were captured using a Zeiss LSM 880 confocal laser scanning microscope with a Plan-Apochromat 10×/0.45, Plan-Apochromat 20×/0.8, C-Apochromat 40×/1.2 WI, and C-Apochromat 63×/1.2 WI objectives. Working concentrations, excitation laser wavelengths, and range of recorded emission wavelengths were as follows: 30 mM, 514 nm, and 566 to 719 nm for propidium iodide; 1 mg mL$^{-1}$, 405 nm, and 410 to 523 nm for Calcouor White; and 0.001% (w/v), 405 nm, and 410 to 535 nm for decolorized Aniline Blue. Pollen was collected from five different plants for each genotype, and the experiment was repeated in two biological replicates.

## Cloning, Complementation Assays and Imaging of GFP-Tagged EXO70A2

All constructs were prepared using the MultiSite Gateway system (Invitrogen). For preparation of the *pEXO70A2::GFP:EXO70A2* and *pEXO70A2::GFP:EXO70A1* constructs, the *EXO70A2* promoter (1,068 bp upstream from the start codon) was subcloned into pENTR 5′-TOPO; the *GFP* gene in pEN-L1-F-L2 was obtained from the Vlaams Instituut voor Biotechnologie (Karimi et al., 2007); the *EXO70A2* (At5g52340) and *EXO70A1* (At5g03540) with stop codons were subcloned into pDONR P2R-P3 using the Gateway BP clonase (Invitrogen). The three elements were then recombined together into the pB7m34GW destination vector (Karimi et al., 2007) using the Gateway LR clonase (Invitrogen).

For cloning of *pEXO70A1::GFP:EXO70A2* and *pEXO70A1::GFP:EXO70A1*, the *EXO70A1* promoter (1 kb upstream from the start codon) was subcloned into pDONR P4-P1r. The *EXO70A1* was subcloned into pDONR P2R-P3. Then, multisite reactions were performed to assemble the *EXO70A1* promoter, GFP, and *EXO70A1* or *EXO70A2* into the destination vector pB7m34GW. The insertions in pDONR vectors were sequenced using M13 primers. The final constructs were sequenced using M13 primers and two GFP primers (see Supplemental Table S1).

*pEXO70A2::GFP:EXO70A2* and *pEXO70A2::GFP:EXO70A1* constructs were then introduced to *exo70a2* heterozygous plants and *pEXO70A1::GFP:EXO70A1* and *pEXO70A1::GFP:EXO70A2* to *exo70a1* heterozygous plants using the *A. tumefaciens*-mediated floral dip method (Clough and Bent, 1998). Transformants were selected by spraying glufosinate solution (BASTA; 150 $mg \cdot L^{-1}$) onto 7-d-old seedlings. Complementation assays were performed using at least two independent transformed lines for each construct.

The subcellular localization of GFP:EXO70A2 in pollen grains, pollen tubes, and roots was performed using a Zeiss LSM 880 confocal laser scanning microscope equipped with a C-Apochromat 63×/1.2 WI. The fluorophore was excitation with a 488-nm laser, and emitted fluorescence was recorded at 493 to 535 nm. The pollen was germinated as described above and carefully transferred to the microscope 2 h after imbibition.

## Accession Numbers

Sequence data from this article can be found in the GenBank/EMBL data libraries under accession numbers 835310 (*EXO70A2*; protein NP_200047.3) and 831809 (*EXO70A1*; protein NP_195974.2).

## Supplemental Data

The following supplemental materials are available.

**Supplemental Figure S1.** Characterization of the *exo70a2* mutant line generated using the CRISPR/Cas9 system.

**Supplemental Figure S2.** Development of wild-type and *exo70a2* pollen.

**Supplemental Figure S3.** Electron microscopic images of cortical regions in wild-type and *exo70a2* pollen grains.

**Supplemental Figure S4.** Visualization of cellulose deposition in slowly growing wild-type pollen tubes in vitro.

**Supplemental Figure S5.** Pollen germination efficiency in the wild type and complemented *exo70a2* mutants at different time points during in vitro germination.

**Supplemental Figure S6.** Morphological parameters of the *exo70a1 exo70a2* double mutant in comparison to *exo70a1* and *exo70a2* single mutants and wild-type plants.

**Supplemental Figure S7.** Analysis of *EXO70A2* expression in the sporophyte.

**Supplemental Figure S8.** Comparison of structural models of EXO70A1 and EXO70A2.

**Supplemental Table S1.** List of primers used in this study.

**Supplemental File S1.** EXO70 sequences used for the phylogenetic analysis.

## ACKNOWLEDGMENTS

We thank Marta Čadyová for technical support, Said Hafidh for technical advice, and Juraj Sekereš for critical reading of the manuscript. Microscopy was performed in the Laboratory of Confocal and Fluorescence Microscopy at the Charles University and in the microscopic department in the Institute of Experimental Botany.

Received October 31, 2019; accepted October 1, 2020; published October 13, 2020.

## LITERATURE CITED

**Abrams ZB, Johnson TS, Huang K, Payne PRO, Coombes K** (2019) A protocol to evaluate RNA sequencing normalization methods. BMC Bioinformatics **20**(Suppl 24): 679

**Alexander MP** (1969) Differential staining of aborted and nonaborted pollen. Stain Technol **44:** 117–122

**Backues SK, Korasick DA, Heese A, Bednarek SY** (2010) The Arabidopsis dynamin-related protein2 family is essential for gametophyte development. Plant Cell **22:** 3218–3231

**Barrett T, Wilhite SE, Ledoux P, Evangelista C, Kim IF, Tomashevsky M, Marshall KA, Phillippy KH, Sherman PM, Holko M, et al** (2013) NCBI GEO: Archive for functional genomics data sets—update. Nucleic Acids Res **41:** D991–D995

**Becker JD, Boavida LC, Carneiro J, Haury M, Feijó JA** (2003) Transcriptional profiling of Arabidopsis tissues reveals the unique characteristics of the pollen transcriptome. Plant Physiol **133:** 713–725

**Beuder S, Dorchak A, Bhide A, Moeller SR, Petersen BL, MacAlister CA** (2020) Exocyst mutants suppress pollen tube growth and cell wall structural defects of hydroxyproline O-arabinosyltransferase mutants. Plant J **103:** 1399–1419

**Bloch D, Pleskot R, Pejchar P, Potocký M, Trpkošová P, Cwiklik L, Vukašinović N, Sternberg H, Yalovsky S, Žárský V** (2016) Exocyst SEC3 and phosphoinositides define sites of exocytosis in pollen tube initiation and growth. Plant Physiol **172:** 980–1002

**Boyd C, Hughes T, Pypaert M, Novick P** (2004) Vesicles carry most exocyst subunits to exocytic sites marked by the remaining two subunits, Sec3p and Exo70p. J Cell Biol **167:** 889–901

**Cai G, Parrotta L, Cresti M** (2015) Organelle trafficking, the cytoskeleton, and pollen tube growth. J Integr Plant Biol **57:** 63–78

**Cankar K, Kortstee A, Toonen MA, Wolters-Arts M, Houbein R, Mariani C, Ulvskov P, Jorgensen B, Schols HA, Visser RG, et al** (2014) Pectic arabinan side chains are essential for pollen cell wall integrity during pollen development. Plant Biotechnol J **12:** 492–502

**Chebli Y, Kaneda M, Zerzour R, Geitmann A** (2012) The cell wall of the Arabidopsis pollen tube—spatial distribution, recycling, and network formation of polysaccharides. Plant Physiol **160:** 1940–1955

**Chebli Y, Kroeger J, Geitmann A** (2013) Transport logistics in pollen tubes. Mol Plant **6:** 1037–1052

**Clough SJ, Bent AF** (1998) Floral dip: A simplified method for *Agrobacterium*-mediated transformation of *Arabidopsis thaliana*. Plant J **16:** 735–743

**Cole RA, Synek L, Zarsky V, Fowler JE** (2005) SEC8, a subunit of the putative Arabidopsis exocyst complex, facilitates pollen germination and competitive pollen tube growth. Plant Physiol **138:** 2005–2018

**Conze LL, Berlin S, Le Bail A, Kost B** (2017) Transcriptome profiling of tobacco (*Nicotiana tabacum*) pollen and pollen tubes. BMC Genomics **18:** 581

**Cvrčková F, Eliáš M, Hála M, Obermeyer G, Žárský V** (2001) Small GTPases and conserved signalling pathways in plant cell morphogenesis: From exocytosis to Exocyst. In A Geitmann, and M Cresti, eds, Cell Biology of Plant and Fungal Tip Growth. IOS Press, Amsterdam, pp 123–136

**Cvrčková F, Grunt M, Bezvoda R, Hála M, Kulich I, Rawat A, Zárský V** (2012) Evolution of the land plant exocyst complexes. Front Plant Sci **3:** 159

**Davidson RM, Gowda M, Moghe G, Lin H, Vaillancourt B, Shiu S-H, Jiang N, Robin Buell C** (2012) Comparative transcriptomics of three Poaceae species reveals patterns of gene expression evolution. Plant J **71:** 492–502

**De Smet R, Sabaghian E, Li Z, Saeys Y, Van de Peer Y** (2017) Coordinated functional divergence of genes after genome duplication in *Arabidopsis thaliana*. Plant Cell **29:** 2786–2800

**Dong G, Hutagalung AH, Fu C, Novick P, Reinisch KM** (2005) The structures of exocyst subunit Exo70p and the Exo84p C-terminal domains reveal a common motif. Nat Struct Mol Biol **12:** 1094–1100

**Drdová EJ, Synek L, Pečenková T, Hála M, Kulich I, Fowler JE, Murphy AS, Zárský V** (2013) The exocyst complex contributes to PIN auxin efflux carrier recycling and polar auxin transport in Arabidopsis. Plant J **73:** 709–719

**Elias M, Drdova E, Ziak D, Bavlnka B, Hala M, Cvrckova F, Soukupova H, Zarsky V** (2003) The exocyst complex in plants. Cell Biol Int **27:** 199–201

**Fendrych M, Synek L, Pecenková T, Drdová EJ, Sekeres J, de Rycke R, Nowack MK, Zársky V** (2013) Visualization of the exocyst complex dynamics at the plasma membrane of *Arabidopsis thaliana*. Mol Biol Cell **24:** 510–520

**Fendrych M, Synek L, Pecenková T, Toupalová H, Cole R, Drdová E, Nebesárová J, Sedinová M, Hála M, Fowler JE, et al** (2010) The Arabidopsis exocyst complex is involved in cytokinesis and cell plate maturation. Plant Cell **22:** 3053–3065

**Ghosh S, Chan C-K** (2016) Analysis of RNA-seq data using TopHat and Cufflinks. *In* D Edwards, ed, Plant Bioinformatics: Methods and Protocols, Methods in Molecular Biology, Vol **1374** Humana Press, New York, pp 339–361

**Goodstein DM, Shu S, Howson R, Neupane R, Hayes RD, Fazo J, Mitros T, Dirks W, Hellsten U, Putnam N, et al** (2012) Phytozome: A comparative platform for green plant genomics. Nucleic Acids Res **40:** D1178–D1186

**Grobei MA, Qeli E, Brunner E, Rehrauer H, Zhang R, Roschitzki B, Basler K, Ahrens CH, Grossniklaus U** (2009) Deterministic protein inference for shotgun proteomics data provides new insights into *Arabidopsis* pollen development and function. Genome Res **19:** 1786–1800

**Guindon S, Dufayard J-F, Lefort V, Anisimova M, Hordijk W, Gascuel O** (2010) New algorithms and methods to estimate maximum-likelihood phylogenies: Assessing the performance of PhyML 3.0. Syst Biol **59:** 307–321

**Guo W, Grant A, Novick P** (1999) Exo84p is an exocyst protein essential for secretion. J Biol Chem **274:** 23558–23564

**Hála M, Cole R, Synek L, Drdová E, Pecenková T, Nordheim A, Lamkemeyer T, Madlung J, Hochholdinger F, Fowler JE, et al** (2008) An exocyst complex functions in plant cell growth in Arabidopsis and tobacco. Plant Cell **20:** 1330–1345

**Hamburger ZA, Hamburger AE, West AP Jr., Weis WI** (2006) Crystal structure of the *S. cerevisiae* exocyst component Exo70p. J Mol Biol **356:** 9–21

**He B, Xi F, Zhang X, Zhang J, Guo W** (2007) Exo70 interacts with phospholipids and mediates the targeting of the exocyst to the plasma membrane. EMBO J **26:** 4053–4065

**Hepler PK, Winship LJ** (2015) The pollen tube clear zone: Clues to the mechanism of polarized growth. J Integr Plant Biol **57:** 79–92

**Hollender C-A, Kang C, Darwish O, Geretz A, Matthews B-F, Slovin J, Alkharouf N, Liu Z** (2014) Floral transcriptomes in woodland strawberry uncover developing receptacle and anther gene networks. Plant Physiol **165:** 1062–1075

**Hong D, Jeon BW, Kim SY, Hwang J-U, Lee Y** (2016) The ROP2-RIC7 pathway negatively regulates light-induced stomatal opening by inhibiting exocyst subunit Exo70B1 in Arabidopsis. New Phytol **209:** 624–635

**Honys D, Twell D** (2003) Comparative analysis of the Arabidopsis pollen transcriptome. Plant Physiol **132:** 640–652

**Hruz T, Laule O, Szabo G, Wessendorp F, Bleuler S, Oertle L, Widmayer P, Gruissem W, Zimmermann P** (2008) Genevestigator v3: A reference expression database for the meta-analysis of transcriptomes. Adv Bioinforma **2008:** 420747

**Hwang JU, Vernoud V, Szumlanski A, Nielsen E, Yang Z** (2008) A tip-localized RhoGAP controls cell polarity by globally inhibiting Rho GTPase at the cell apex. Curr Biol **18:** 1907–1916

**Janková Drdová E, Klejchová M, Janko K, Hála M, Soukupová H, Cvrčková F, Žárský V** (2019) Developmental plasticity of *Arabidopsis* hypocotyl is dependent on exocyst complex function. J Exp Bot **70:** 1255–1265

**Jiang L, Yang S-L, Xie L-F, Puah CS, Zhang X-Q, Yang W-C, Sundaresan V, Ye D** (2005) VANGUARD1 encodes a pectin methylesterase that enhances pollen tube growth in the *Arabidopsis* style and transmitting tract. Plant Cell **17:** 584–596

**Johnson MA, Preuss D** (2002) Plotting a course: Multiple signals guide pollen tubes to their targets. Dev Cell **2:** 273–281

**Kang B-H, Rancour DM, Bednarek SY** (2003) The dynamin-like protein ADL1C is essential for plasma membrane maintenance during pollen maturation. Plant J **35:** 1–15

**Karimi M, Bleys A, Vanderhaeghen R, Hilson P** (2007) Building blocks for plant gene assembly. Plant Physiol **145:** 1183–1191

**Katoh K, Standley DM** (2013) MAFFT multiple sequence alignment software version 7: Improvements in performance and usability. Mol Biol Evol **30:** 772–780

**Kaya H, Iwano M, Takeda S, Kanaoka MM, Kimura S, Abe M, Kuchitsu K** (2015) Apoplastic ROS production upon pollination by RbohH and RbohJ in Arabidopsis. Plant Signal Behav **10:** e989050

**Kubátová Z, Pejchar P, Potocký M, Sekereš J, Žárský V, Kulich I** (2019) *Arabidopsis* trichome contains two plasma membrane domains with different lipid compositions which attract distinct EXO70 subunits. Int J Mol Sci **20:** 3803

**Kulich I, Cole R, Drdová E, Cvrcková F, Soukup A, Fowler J, Zárský V** (2010) Arabidopsis exocyst subunits SEC8 and EXO70A1 and exocyst interactor ROH1 are involved in the localized deposition of seed coat pectin. New Phytol **188:** 615–625

**Kulich I, Pečenková T, Sekereš J, Smetana O, Fendrych M, Foissner I, Höftberger M, Zárský V** (2013) Arabidopsis exocyst subcomplex containing subunit EXO70B1 is involved in autophagy-related transport to the vacuole. Traffic **14:** 1155–1165

**Kulich I, Vojtíková Z, Glanc M, Ortmannová J, Rasmann S, Žárský V** (2015) Cell wall maturation of Arabidopsis trichomes is dependent on exocyst subunit EXO70H4 and involves callose deposition. Plant Physiol **168:** 120–131

**Lassig R, Gutermuth T, Bey TD, Konrad KR, Romeis T** (2014) Pollen tube NAD(P)H oxidases act as a speed control to dampen growth rate oscillations during polarized cell growth. Plant J **78:** 94–106

**Lavy M, Bloch D, Hazak O, Gutman I, Poraty L, Sorek N, Sternberg H, Yalovsky S** (2007) A Novel ROP/RAC effector links cell polarity, root-meristem maintenance, and vesicle trafficking. Curr Biol **17:** 947–952

**Leroux C, Bouton S, Kiefer-Meyer M-C, Fabrice TN, Mareck A, Guénin S, Fournet F, Ringli C, Pelloux J, Driouich A, et al** (2015) PECTIN METHYLESTERASE48 is involved in Arabidopsis pollen grain germination. Plant Physiol **167:** 367–380

**Li S, Gu Y, Yan A, Lord E, Yang ZB** (2008) RIP1 (ROP Interactive Partner 1)/ICR1 marks pollen germination sites and may act in the ROP1 pathway in the control of polarized pollen growth. Mol Plant **1:** 1021–1035

**Loraine AE, McCormick S, Estrada A, Patel K, Qin P** (2013) RNA-seq of Arabidopsis pollen uncovers novel transcription and alternative splicing. Plant Physiol **162:** 1092–1109

**MacAlister CA, Ortiz-Ramírez C, Becker JD, Feijó JA, Lippman ZB** (2016) Hydroxyproline O-arabinosyltransferase mutants oppositely alter tip growth in *Arabidopsis thaliana* and *Physcomitrella patens*. Plant J **85:** 193–208

**Matern HT, Yeaman C, Nelson WJ, Scheller RH** (2001) The Sec6/8 complex in mammalian cells: Characterization of mammalian Sec3, subunit interactions, and expression of subunits in polarized cells. Proc Natl Acad Sci USA **98:** 9648–9653

**Mei K, Li Y, Wang S, Shao G, Wang J, Ding Y, Luo G, Yue P, Liu JJ, Wang X, et al** (2018) Cryo-EM structure of the exocyst complex. Nat Struct Mol Biol **25:** 139–146

**Mori T, Kuroiwa H, Higashiyama T, Kuroiwa T** (2006) GENERATIVE CELL SPECIFIC 1 is essential for angiosperm fertilization. Nat Cell Biol **8:** 64–71

**Paul P, Röth S, Schleiff E** (2016) Importance of organellar proteins, protein translocation and vesicle transport routes for pollen development and function. Plant Reprod **29:** 53–65

**Pečenková T, Hála M, Kulich I, Kocourková D, Drdová E, Fendrych M, Toupalová H, Zárský V** (2011) The role for the exocyst complex subunits Exo70B2 and Exo70H1 in the plant-pathogen interaction. J Exp Bot **62:** 2107–2116

**Pečenková T, Markovic V, Sabol P, Kulich I, Žárský V** (2017) Exocyst and autophagy-related membrane trafficking in plants. J Exp Bot **69:** 47–57

**Peng J, Ilarslan H, Wurtele ES, Bassham DC** (2011) AtRabD2b and AtRabD2c have overlapping functions in pollen development and pollen tube growth. BMC Plant Biol **11:** 25

**Pleskot R, Cwiklik L, Jungwirth P, Žárský V, Potocký M** (2015) Membrane targeting of the yeast exocyst complex. Biochim Biophys Acta **1848:** 1481–1489

**Potocký M, Jones MA, Bezvoda R, Smirnoff N, Zárský V** (2007) Reactive oxygen species produced by NADPH oxidase are involved in pollen tube growth. New Phytol **174:** 742–751

**Potocký M, Pejchar P, Gutkowska M, Jiménez-Quesada MJ, Potocká A, Alché J de D, Kost B, Žárský V** (2012) NADPH oxidase activity in pollen tubes is affected by calcium ions, signaling phospholipids and Rac/Rop GTPases. J Plant Physiol **169:** 1654–1663

**Proost S, Mutwil M** (2018) CoNekT: An open-source framework for comparative genomic and transcriptomic network analyses. Nucleic Acids Res **46**(W1): W133–W140

**Qin Y, Dong J** (2015) Focusing on the focus: What else beyond the master switches for polar cell growth? Mol Plant **8:** 582–594

**Rawat A, Brejšková L, Hála M, Cvrčková F, Žárský V** (2017) The *Physcomitrella patens* exocyst subunit EXO70.3d has distinct roles in growth and development, and is essential for completion of the moss life cycle. New Phytol **216:** 438–454

**Ronquist F, Teslenko M, van der Mark P, Ayres DL, Darling A, Höhna S, Larget B, Liu L, Suchard MA, Huelsenbeck JP** (2012) MrBayes 3.2: Efficient Bayesian phylogenetic inference and model choice across a large model space. Syst Biol **61:** 539–542

**Rossetti S, Bonatti PM** (2001) In situ histochemical monitoring of ozone- and TMV-induced reactive oxygen species in tobacco leaves. Plant Physiol Biochem **39:** 433–442

**Rybak K, Steiner A, Synek L, Klaeger S, Kulich I, Facher E, Wanner G, Kuster B, Zarsky V, Persson S, et al** (2014) Plant cytokinesis is orchestrated by the sequential action of the TRAPPII and exocyst tethering complexes. Dev Cell **29:** 607–620

**Sabol P, Kulich I, Žárský V** (2017) RIN4 recruits the exocyst subunit EXO70B1 to the plasma membrane. J Exp Bot **68:** 3253–3265

**Sekereš J, Pejchar P, Šantrůček J, Vukašinović N, Žárský V, Potocký M** (2017) Analysis of exocyst subunit EXO70 family reveals distinct membrane polar domains in tobacco pollen tubes. Plant Physiol **173:** 1659–1675

**Smirnova AV, Matveyeva NP, Yermakov IP** (2014) Reactive oxygen species are involved in regulation of pollen wall cytomechanics. Plant Biol **16:** 252–257

**Synek L, Schlager N, Eliás M, Quentin M, Hauser M-T, Zárský V** (2006) AtEXO70A1, a member of a family of putative exocyst subunits specifically expanded in land plants, is important for polar growth and plant development. Plant J **48:** 54–72

**Synek L, Vukašinović N, Kulich I, Hála M, Aldorfová K, Fendrych M, Žárský V** (2017) EXO70C2 is a key regulatory factor for optimal tip growth of pollen. Plant Physiol **174:** 223–240

**TerBush DR, Maurice T, Roth D, Novick P** (1996) The exocyst is a multiprotein complex required for exocytosis in *Saccharomyces cerevisiae*. EMBO J **15:** 6483–6494

**Tian G-W, Chen M-H, Zaltsman A, Citovsky V** (2006) Pollen-specific pectin methylesterase involved in pollen tube growth. Dev Biol **294:** 83–91

**Vogler F, Schmalzl C, Englhart M, Bircheneder M, Sprunck S** (2014) Brassinosteroids promote Arabidopsis pollen germination and growth. Plant Reprod **27:** 153–167

**Vukašinović N, Cvrčková F, Eliáš M, Cole R, Fowler JE, Žárský V, Synek L** (2014) Dissecting a hidden gene duplication: The *Arabidopsis thaliana* SEC10 locus. PLoS One **9:** e94077

**Vukašinović N, Oda Y, Pejchar P, Synek L, Pečenková T, Rawat A, Sekereš J, Potocký M, Žárský V** (2017) Microtubule-dependent targeting of the exocyst complex is necessary for xylem development in *Arabidopsis*. New Phytol **213:** 1052–1067

**Wang X, Wang K, Yin G, Liu X, Liu M, Cao N, Duan Y, Gao H, Wang W, Ge W, et al** (2018) Pollen-expressed leucine-rich repeat extensins are essential for pollen germination and growth. Plant Physiol **176:** 1993–2006

**Wang Z-P, Xing H-L, Dong L, Zhang H-Y, Han C-Y, Wang X-C, Chen Q-J** (2015) Egg cell-specific promoter-controlled CRISPR/Cas9 efficiently generates homozygous mutants for multiple target genes in *Arabidopsis* in a single generation. Genome Biol **16:** 144

**Waterhouse AM, Procter JB, Martin DMA, Clamp M, Barton GJ** (2009) Jalview Version 2—a multiple sequence alignment editor and analysis workbench. Bioinformatics **25:** 1189–1191

**Žárský V, Kulich I, Fendrych M, Pečenková T** (2013) Exocyst complexes multiple functions in plant cells secretory pathways. Curr Opin Plant Biol **16:** 726–733

**Žárský V, Sekereš J, Kubátová Z, Pečenková T, Cvrčková F** (2020) Three subfamilies of exocyst EXO70 family subunits in land plants: Early divergence and ongoing functional specialization. J Exp Bot **71:** 49–62

**Zhang C, Brown MQ, van de Ven W, Zhang ZM, Wu B, Young MC, Synek L, Borchardt D, Harrison R, Pan S, et al** (2016) Endosidin2 targets conserved exocyst complex subunit EXO70 to inhibit exocytosis. Proc Natl Acad Sci USA **113:** E41–E50

**Zhang X, Pumplin N, Ivanov S, Harrison MJ** (2015) EXO70I is required for development of a sub-domain of the periarbuscular membrane during arbuscular mycorrhizal symbiosis. Curr Biol **25:** 2189–2195

**Zhao L-J, Yuan H-M, Guo W-D, Yang C-P** (2016) Digital gene expression analysis of *Populus simonii* × *P. nigra* pollen germination and tube growth. Front Plant Sci **7:** 825

**Zhou H, Yin H, Chen J, Liu X, Gao Y, Wu J, Zhang S** (2016) Gene-expression profile of developing pollen tube of *Pyrus bretschneideri*. Gene Expr Patterns **20:** 11–21